Axions (A^0) and Other Very Light Bosons, Searches for

AXIONS

Written in August 2007 by C. Hagmann (LLNL), H. Murayama (UC Berkeley), G.G. Raffelt (MPI Physics), L.J. Rosenberg (U. of Washington), and K. van Bibber (LLNL).

Introduction: In this section, we list mass and coupling-strength limits for very light neutral scalar or pseudoscalar bosons that couple weakly to normal matter and radiation. Such bosons may arise from a global spontaneously broken U(1) symmetry, resulting in a massless Nambu-Goldstone (NG) boson. If there is a small explicit symmetry breaking, either already in the Lagrangian or due to quantum-mechanical effects such as anomalies, the boson acquires a mass and is called a pseudo-NG boson. Typical examples are axions (A^0) [1,2], familons [3] and Majorons [4], associated, respectively, with a spontaneously broken Peccei-Quinn, family and lepton-number symmetry.

A common characteristic among these light bosons ϕ is that their coupling to Standard-Model particles is suppressed by the energy scale that characterizes the symmetry breaking, *i.e.*, the decay constant f. The interaction Lagrangian is

$$\mathcal{L} = f^{-1} J^{\mu} \partial_{\mu} \phi \,, \tag{1}$$

where J^{μ} is the Noether current of the spontaneously broken global symmetry. If f is very large, these new particles interact very weakly. Conversely, detecting them would provide a window to physics far beyond what can be probed at accelerators.

The interest in global symmetries and the associated NG bosons has somewhat waned except for the case of axions where it has held steady since they were proposed 30 years ago. This is because the Peccei-Quinn (PQ) mechanism remains perhaps the most credible scheme to preserve CP in QCD; axions are a plausible candidate for the cold dark matter of the universe and they are searched for in experiments with a realistic chance of discovery. Originally it was assumed that the PQ scale f_A was related to the electroweak symmetry-breaking scale $v_{\rm weak} = (\sqrt{2}G_{\rm F})^{-1/2} = 247$ GeV. However, the associated "standard" and "variant" axions were quickly excluded, leaving "invisible axions" with $f_A \gg v_{\rm weak}$ as the main possibility. We refer to the Listings for limits on standard and variant axions, whereas here we focus primarily on very low-mass, very weakly-interacting axions and axion-like particles.

I. THEORY

I.1 Peccei-Quinn mechanism and axions: QCD includes a CP-violating Lagrangian $\mathcal{L}_{\Theta} = \bar{\Theta}\,(\alpha_s/8\pi)\, G^{\mu\nu a}\tilde{G}^{a}_{\mu\nu}$, where $-\pi \leq \bar{\Theta} \leq +\pi$ is the effective Θ parameter after diagonalization of the quark masses, G is the color field strength tensor, and $\tilde{G}$ its dual. Experimental limits on the neutron electric dipole moment [5] imply $|\bar{\Theta}| \lesssim 10^{-10}$ even though $\bar{\Theta} = \mathcal{O}(1)$ is otherwise completely satisfactory. The spontaneously broken global Peccei-Quinn symmetry $\mathrm{U(1)_{PQ}}$ was introduced to solve this "strong CP problem" [1], and an axion is the pseudo-NG boson of $\mathrm{U(1)_{PQ}}$ [2]. This symmetry is exact on the classical level, but is broken quantum mechanically due to the axion's anomalous triangle coupling to gluons,

$$\mathcal{L} = \left(\bar{\Theta} - \frac{\phi_A}{f_A}\right) \frac{\alpha_s}{8\pi}\, G^{\mu\nu a}\tilde{G}^{a}_{\mu\nu} \,, \tag{2}$$

where ϕ_A is the axion field and f_A the axion decay constant. Color anomaly factors have been absorbed in the normalization of f_A which is defined by this Lagrangian. Thus normalized, f_A is the quantity that enters all low-energy phenomena [6]. Non-perturbative effects induce a potential for ϕ_A whose minimum is at $\phi_A = \bar{\Theta}\, f_A$, thereby canceling the $\bar{\Theta}$ term in the QCD Lagrangian, and thus restoring the CP symmetry.

The resulting axion mass is given by $m_A f_A \approx m_\pi f_\pi$ where $m_\pi = 135$ MeV and $f_\pi \approx 92$ MeV is the pion decay constant. In more detail one finds

$$m_A = \frac{z^{1/2}}{1+z}\,\frac{f_\pi m_\pi}{f_A} = \frac{0.60\ \text{meV}}{f_A/10^{10}\,\text{GeV}} \,, \tag{3}$$

where $z = m_u/m_d$ is the up/down quark-mass ratio. For this numerical estimate we used a canonical value of $z = 0.56$ [7], but it could vary in the range $z = 0.3$–0.6 [8].

In the original axion model, $f_A \sim v_{\rm weak}$ [1,2]. Tree-level flavor conservation fixes the axion mass and its couplings in terms of a single parameter $\tan\beta$, the ratio of the vacuum expectation values of the two Higgs fields that appear as a minimal ingredient. This "standard axion" is excluded after extensive experimental searches [9]. A reported observation of a narrow-peak structure in positron spectra from heavy ion collisions [10] suggested an axion-like particle of mass 1.8 MeV that decays into e^+e^-, but extensive searches for the A^0(1.8 MeV) ended negative. "Variant axion models" were proposed which keep $f_A \sim v_{\rm weak}$ while dropping the constraint of tree-level flavor conservation [11], but these models are also excluded [12].

Axions with $f_A \gg v_{\rm weak}$ evade all existing experimental limits. Two classes of models are often discussed in the literature. In "hadronic axion models," one introduces new heavy quarks carrying the $\mathrm{U(1)_{PQ}}$ charge, leaving the usual quarks and leptons without any tree-level axion couplings. The prototype is the KSVZ model [13], which has the additional property that the heavy quarks are electrically neutral. Another model class simply requires a minimum of two Higgs doublets with the usual quarks and leptons carrying PQ charges, the prototype being the DFSZ model [14]. All of these models contain at least one electroweak singlet scalar boson, which acquires a vacuum expectation value and thereby breaks the PQ symmetry. The KSVZ and DFSZ models are frequently used as generic examples, but other models exist where both heavy quarks and Higgs doublets carry PQ charges. In one recent example, the PQ charges of all fields were derived within a superstring model [15].

I.2 Model-dependent axion couplings: Although the generic axion interactions scale approximately with f_π/f_A from the corresponding π^0 couplings, there are non-negligible model-dependent factors and uncertainties. The axion's two-photon interaction plays a key role for many searches,

$$\mathcal{L}_{A\gamma\gamma} = \frac{G_{A\gamma\gamma}}{4} F_{\mu\nu}\tilde{F}^{\mu\nu}\phi_A = -G_{A\gamma\gamma}\mathbf{E}\cdot\mathbf{B}\,\phi_A\,. \quad (4)$$

Here, F is the electromagnetic field-strength tensor, $\tilde{F}$ its dual, and $\mathbf{E}$ and $\mathbf{B}$ the electric and magnetic fields, respectively. The coupling constant is

$$\begin{aligned} G_{A\gamma\gamma} &= \frac{\alpha}{2\pi f_A}\left(\frac{E}{N} - \frac{2}{3}\frac{4+z}{1+z}\right) \\ &= \frac{\alpha}{2\pi}\left(\frac{E}{N} - \frac{2}{3}\frac{4+z}{1+z}\right)\frac{1+z}{z^{1/2}}\frac{m_A}{m_\pi f_\pi}\,, \end{aligned} \quad (5)$$

where E and N, respectively, are the electromagnetic and color anomalies of the axial current associated with the axion. In grand unified models, and notably in the DFSZ case [14], we have $E/N = 8/3$, whereas $E/N = 0$ for KSVZ [13] if the electric charge of the new heavy quark is taken to vanish. However, in general, E/N is not known so that for fixed f_A, a broad range of $G_{A\gamma\gamma}$ values is possible [16].

Axions or axion-like particles with a two-photon vertex decay with a rate

$$\begin{aligned} \Gamma_{A\to\gamma\gamma} &= \frac{G^2_{A\gamma\gamma}m_A^3}{64\,\pi} \\ &= \frac{\alpha^2}{256\,\pi^3}\left(\frac{E}{N} - \frac{2}{3}\frac{4+z}{1+z}\right)^2\frac{(1+z)^2}{z}\frac{m_A^5}{m_\pi^2 f_\pi^2} \\ &= 1.1\times 10^{-24}\ \mathrm{s}^{-1}\left(\frac{m_A}{\mathrm{eV}}\right)^5, \end{aligned} \quad (6)$$

where the first expression is for general pseudoscalars, the second for axions, and the third assumes $z = 0.56$ and $E/N = 0$. Axions decay faster than the age of the universe if $m_A \gtrsim 20$ eV.

The interaction with fermions f has a derivative structure so that it is invariant under a constant shift $\phi_A \to \phi_A + \phi_0$ as behooves a NG boson,

$$\mathcal{L}_{Aff} = \frac{C_f}{2f_A}\bar{\Psi}_f\gamma^\mu\gamma_5\Psi_f\partial_\mu\phi_A \quad \text{or} \quad -\mathrm{i}\frac{C_f m_f}{f_A}\bar{\Psi}_f\gamma_5\Psi_f\phi_A\,. \quad (7)$$

Here, Ψ_f is the fermion field, m_f its mass, and C_f a model-dependent numerical coefficient. The dimensionless combination $g_{Aff} \equiv C_f m_f/f_A$ plays the role of a Yukawa coupling and $\alpha_{Aff} \equiv g^2_{Aff}/4\pi$ of a "fine-structure constant." The pseudoscalar form is usually equivalent to the derivative structure, but one has to be careful in processes where two NG bosons are attached to one fermion line, for example in the context of axion emission by nucleon bremsstrahlung [17].

Hadronic axions do not couple to ordinary quarks and leptons at tree level. In the DFSZ model [14], the coupling coefficient to electrons is

$$C_e = \frac{\cos^2\beta}{3}\,, \quad (8)$$

where $\tan\beta$ is the ratio of two Higgs vacuum expectation values that are generic to this and similar models.

The nucleon couplings $C_{n,p}$ are related to nucleon axial-vector current matrix elements by generalized Goldberger-Treiman relations,

$$\begin{aligned} C_p &= (C_u-\eta)\Delta u + (C_d-\eta z)\Delta d + (C_s-\eta w)\Delta s\,, \\ C_n &= (C_u-\eta)\Delta d + (C_d-\eta z)\Delta u + (C_s-\eta w)\Delta s\,. \end{aligned} \quad (9)$$

Here, $\eta = (1+z+w)^{-1}$ with $z = m_u/m_d$ and $w = m_u/m_s \ll z$. Δq represents the axial-vector current couplings to the proton by $\Delta q\, S_\mu = \langle p|\bar{q}\gamma_\mu\gamma_5 q|p\rangle$, where S_μ is the proton spin.

Neutron beta decay and strong isospin symmetry considerations imply $\Delta u - \Delta d = F + D = 1.267\pm 0.0035$, whereas hyperon decays and flavor SU(3) symmetry imply $\Delta u + \Delta d - 2\Delta s = 3F - D = 0.585 \pm 0.025$. The strange-quark contribution is $\Delta s = -0.08 \pm 0.01_{\rm stat} \pm 0.05_{\rm syst}$ from the COMPASS experiment [18], and $\Delta s = -0.085 \pm 0.008_{\rm exp} \pm 0.013_{\rm theor} \pm 0.009_{\rm evol}$ from HERMES [19], in agreement with each other and with an early estimate of $\Delta s = -0.11 \pm 0.03$ [20]. We thus adopt

$$\begin{aligned} \Delta u &= +0.841 \pm 0.020\,, \\ \Delta d &= -0.426 \pm 0.020\,, \\ \Delta s &= -0.085 \pm 0.015\,, \end{aligned} \quad (10)$$

which are very similar to what was used in the axion literature.

The uncertainty of the axion-nucleon couplings is dominated by the uncertainty $z = 0.3$–0.6 that we mentioned earlier. For hadronic axions $C_{u,d,s} = 0$, so that $C_p = -0.55$ and $C_n = +0.14$, if $z = 0.3$ and $C_p = -0.37$ and $C_n = -0.05$ if $z = 0.6$. While it is well possible that $C_n = 0$, C_p does not vanish within the plausible z range. In the DFSZ model, $C_u = \frac{1}{3}\sin^2\beta$ and $C_d = \frac{1}{3}\cos^2\beta$. Even with the large z–uncertainty, C_n and C_p never vanish simultaneously. An extreme case is $\cos^2\beta = 0$, where $C_p = 0$ for $z = 0.3$, but in this case $C_n = -0.27$.

The axion–pion interaction is given by the Lagrangian [21]

$$\mathcal{L}_{A\pi} = \frac{C_{A\pi}}{f_\pi f_A}\left(\pi^0\pi^+\partial_\mu\pi^- + \pi^0\pi^-\partial_\mu\pi^+ - 2\pi^+\pi^-\partial_\mu\pi^0\right)\partial_\mu\phi_A\,. \quad (11)$$

In hadronic axion models, the coupling constant is

$$C_{A\pi} = \frac{1-z}{3(1+z)}\,. \quad (12)$$

In general the chiral symmetry-breaking Lagrangian contributes an additional piece to $\mathcal{L}_{A\pi}$ proportional to $(m_\pi^2/f_\pi f_A)\,(\pi^0\pi^0 + 2\pi^-\pi^+)\,\pi^0\phi_A$. For hadronic axions, this term vanishes identically, in contrast, for example, to the DFSZ model (Roberto Peccei, private communication).

II. LABORATORY SEARCHES

II.1 Photon regeneration: Searching for "invisible axions" in laboratory experiments is extremely challenging. The most promising approaches use the axion-two-photon vertex, allowing axions and photons to convert into each other in the presence of external electric or magnetic fields [22]. When the external field is the Coulomb field of a charged particle, the conversion is best viewed as an ordinary scattering process, $\gamma + Ze \leftrightarrow Ze + A$, called Primakoff effect in analogy to the corresponding π^0 process [23]. In the other extreme of a macroscopic field, usually a large-scale B–field, the momentum transfer is small, the interaction coherent over a large distance, and the conversion is best viewed as an axion–photon oscillation phenomenon in analogy to neutrino-flavor oscillations [24]. The search for solar axions with the "helioscope technique" [22], or for dark-matter axions with the "haloscope technique" [22], are based on this concept and will be discussed in the sections on stellar and cosmological axions below, whereas here we concentrate on pure laboratory experiments that do not require astrophysical sources.

Photons propagating through a transverse magnetic field, with incident **E** and magnet **B** parallel, may convert into axions. For light axions with $m_A^2 L/2\omega \ll 2\pi$, where L is the length of the magnetic field conversion region and ω the photon energy, the resultant axion beam is collinear and coherent with the incident photon beam, and the conversion probability Π is given by $\Pi \sim (1/4)(G_{A\gamma\gamma}BL)^2$. A practical realization of this concept is a laser beam propagating down the bore of a long superconducting dipole magnet (like the bending magnets in high-energy accelerators). If another such dipole magnet is in line with the first, with an optical barrier separating the two, then photons may be regenerated and detected in the second magnet from the pure axion beam [25]. The overall probability $P(\gamma \to A \to \gamma) = \Pi^2$.

Such an experiment has been carried out, utilizing two magnets of length $L = 4.4$ m and $B = 3.7$ T. For $m_A <$ 1 meV, the coupling was found to be constrained by $G_{A\gamma\gamma} < 6.7 \times 10^{-7}$ GeV^{-1} at 95% CL [26]. More recently, the Light Pseudo Scalar Search project (LIPSS) collaboration has taken data at the Jefferson Laboratory free-electron infrared laser facility. The claimed sensitivity of their detector is $G_{A\gamma\gamma} = 1.7 \times 10^{-6}$ GeV^{-1} [27]. Another recent experiment uses a pulsed laser with similar sensitivity [28]. Most recently, the GammeV Particle Search Experiment experiment at FNAL has reported a 3σ constraint of $G_{A\gamma\gamma} < 3.2 \times 10^{-7}$ GeV^{-1} in the limit $m_A = 0$ [29]. Other experiments that are planned or under construction include the Axion-Like Particle Search experiment (ALPS) at DESY, and the Optical Search for QED vacuum magnetic birefringence experiment at CERN.

A new concept has been proposed, resonantly-enhanced photon regeneration, which may enable searches into unexplored regions of axion-photon couplings [30]. In this scheme, both the production and detection magnets are within Fabry-Perot optical cavities and actively locked in frequency. The enhancement is $P^{\rm res}(\gamma \to a \to \gamma) = (2\mathcal{F}\mathcal{F}'/\pi^2) \times P^{\rm non-res}$, where $\mathcal{F}$ and $\mathcal{F}'$ are the finesse of the two optical cavities. Feasibly, the resonant enhancement could be of order $10^{(10-12)}$, leading to improvements in sensitivity in $G_{A\gamma\gamma}$ of $10^{(2.5-3)}$.

II.2 Photon polarization: An alternative to regenerating the lost photons is to use the beam itself to detect the B-field-induced photon-axion conversion: the polarization of light propagating through a transverse magnetic field suffers dichroism and birefrigence [31]. Dichroism: The $E_\parallel$ component, but not the $E_\perp$ component, will be depleted by the production of axions, and thus there will be in general a small rotation of the polarization vector of linearly-polarized light. The effect will be constant for all sufficiently light axions, such that the oscillation length is much longer than the magnet $m_A^2 L/2\omega \ll 2\pi$. For heavier axions, the effect oscillates and diminishes as m_A increases, and vanishes for $m_A > \omega$. Birefrigence: This rotation occurs because there is mixing of virtual axions in the $E_\parallel$ state, but not for the $E_\perp$ state. Hence, initially linearly polarized light will become elliptically polarized. Higher-order QED also induces vacuum birefrigence. A search for these effects was performed on the same dipole magnets in the early experiment above [32]. Any effect increases linearly when the beam passes through an optical cavity within the magnet. The dichroic rotation gave a stronger limit than the ellipticity rotation: $G_{A\gamma\gamma} < 3.6 \times 10^{-7}$ GeV^{-1} at 95% CL for $m_A < 5 \times 10^{-4}$ eV. The ellipticity rotation limits are better at higher masses, as they fall off smoothly and do not terminate at m_A.

In 2006, a publication by the PVLAS collaboration reported a signature of magnetically induced vacuum dichroism, which could have been interpreted as evidence for a light pseudoscalar with a mass of 1–1.5 meV and a photon coupling of $(1.6\text{–}5) \times 10^{-6}$ GeV^{-1} [33]. This result was problematic from several points of view, not the least of which was the difficulty in reconciling the magnitude of the signal with the much more restrictive limits on $G_{A\gamma\gamma}$ from the Sun, horizontal branch stars, and CAST (see below). Furthermore, the PVLAS data themselves evidenced large systematic errors of unknown origin. More recently, the PVLAS collaboration issued a report retracting their earlier findings. They conclude the effects were instrumental artifacts, with no evidence for new physics [34].

II.3 Long-range forces: New bosons would mediate long-range forces, which are severely constrained by "fifth force" experiments [35]. These experiments, notably those looking for new mass-spin couplings, provide significant constraints on axion-like particles [36,37]. The limits on the product of couplings at the mass- and spin-coupled interaction vertices (Figure 1) may be related to limits on the DFSZ model [36].

In summary, pure laboratory searches for invisible axions have not yet provided useful limits on plausible models. Photon propagation or long-range force experiments are only sensitive for small m_A, so that the corresponding coupling strengths that scale with $f_A^{-1} \approx m_A/m_\pi f_\pi$ are too small to be detected. However, these efforts provide constraints on general low-mass bosons, and have searched for axions of non-standard masses and couplings.

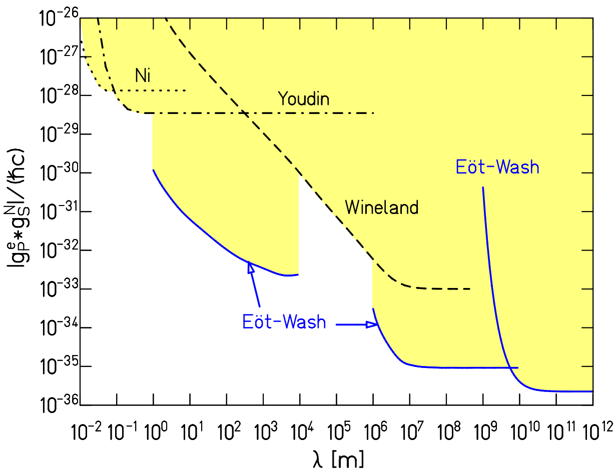

Figure 1: Short-distance gravity upper limits [37] on the product of mass- and spin-vertex couplings as a function of the interaction range λ; the shaded region is excluded at 95% confidence. Figure courtesy E. Adelberger.

III. AXIONS FROM ASTROPHYSICAL SOURCES

III.1 Stellar energy-loss limits: Low-mass weakly-interacting particles (neutrinos, gravitons, axions, baryonic or leptonic gauge bosons, *etc.*) are produced in hot astrophysical plasmas, and can thus transport energy out of stars. The coupling strength of the particles with normal matter and radiation is bounded by the constraint that stellar-evolution lifetimes or energy-loss rates not conflict with observation [38–40].

We begin with our Sun and concentrate on hadronic axion models. The dominant production is by the Primakoff process $\gamma + Ze \to Ze + A$, where photons convert into axions in the electric fields of the charged particles in the plasma. Integrating over a standard solar model, one finds an axion luminosity [53]

$$L_A = G_{10}^2\, 1.85 \times 10^{-3}\, L_\odot\,, \qquad (13)$$

where $G_{10} = G_{A\gamma\gamma} \times 10^{10}$ GeV. The maximum of the spectrum is at 3.0 keV, the average at 4.2 keV, and the number flux at Earth is G_{10}^2 3.75×10^{11} cm^{-2} s^{-1}.

The axion losses lead to an enhanced consumption of nuclear fuel. The standard Sun is halfway through its hydrogen-burning phase so that the solar axion luminosity cannot significantly exceed its photon luminosity $L_\odot$. For a more refined constraint, we note that a model of the present-day Sun, with the integrated effect of axion losses taken into account, differs from a standard solar model for sufficiently large values of the coupling constant. The modified sound-speed profile can be diagnosed by helioseismology, providing a conservative limit $G_{10} \lesssim 10$, corresponding to $L_A \lesssim 0.20\, L_\odot$ [41]. More recent determinations of the solar metal abundances have spoiled the almost perfect agreement between standard solar models and helioseismology [42], a problem that is not yet resolved. However, the axion limit probably remains unaffected.

The energy loss by solar axion emission requires enhanced nuclear burning, and thus an increased temperature. Self-consistent solar models with axion losses reveal that $G_{10} = 4.5$ causes a 20% increase of the solar ^{8}B neutrino flux [41]. The measured all-flavor ^{8}B solar neutrino flux is 4.94×10^6 cm^{-2} s^{-1} with an uncertainty of about 8.8% [43]. The old standard solar model predictions were 5.7–5.9 in the same units, whereas the new metal abundances imply 4.5–4.6, each time with a 16% "theoretical 1σ error" [42]. Therefore, the measured neutrino fluxes imply a limit $G_{10} \lesssim 5$, corresponding to $L_A \lesssim 0.04\, L_\odot$.

A more restrictive limit on $G_{A\gamma\gamma}$ arises from globular-cluster (GC) stars. A GC is a gravitationally bound system of a homogeneous population of low-mass stars, allowing for detailed tests of stellar-evolution theory. The stars on the horizontal branch (HB) in the color-magnitude diagram have reached helium burning, where their core (mass $\sim 0.5\, M_\odot$, density $\sim 10^4$ g cm^{-3}, temperature $\sim 10^8$ K) generates energy by fusing helium to carbon and oxygen with a core-averaged energy release of about 80 erg g^{-1} s^{-1}. The core-averaged Primakoff axion loss rate is about $G_{10}^2\, 30$ erg g^{-1} s^{-1}. The main effect is accelerated consumption of helium, and thus a reduction of the HB lifetime by about $80/(80 + 30\, G_{10}^2)$. The HB lifetime is measured relative to the red-giant branch (RGB) evolutionary time scale by comparing the number of HB stars with the number of RGB stars. This number ratio agrees with expectations within 20–40% in any one of 15 studied GCs [44]. Compounding the results of all 15 GCs, the agreement is within about 10% [39]. A reasonably conservative limit is

$$G_{A\gamma\gamma} \lesssim 1 \times 10^{-10}\ \text{GeV}^{-1}\,, \qquad (14)$$

although an objective error budget is not available.

We translate this nominal constraint on the axion-photon interaction strength to $f_A > 2.3 \times 10^7$ GeV (and thus $m_A < 0.3$ eV), using $z = 0.56$ and $E/N = 0$ as in the KSVZ model, and show the excluded range in Figure 2. For the DFSZ model with $E/N = 8/3$, the corresponding limits are slightly less restrictive, $f_A > 0.8 \times 10^7$ GeV (and thus $m_A < 0.7$ eV). The exact high-mass end of the exclusion range has not been determined. We note that the relevant temperature is around 10 keV, and the average photon energy is therefore around 30 keV. The excluded m_A range thus certainly extends beyond the shown 100 keV.

In models where axions couple directly to electrons, processes of the form $\gamma + e^- \to e^- + a$ and $e^- + Ze \to Ze + e^- + a$ are more efficient than the Primakoff process. Moreover, bremsstrahlung is efficient in degenerate stars such as white dwarfs, where the Primakoff and Compton processes are suppressed by the large photon plasma frequency. One limit comes from GC stars where the enhanced energy losses would delay helium ignition so that the tip of the RGB would be brighter than observed [45], implying $\alpha_{Aee} \lesssim 0.5 \times 10^{-26}$. Axion emission would also enhance white-dwarf cooling, leading to a similar

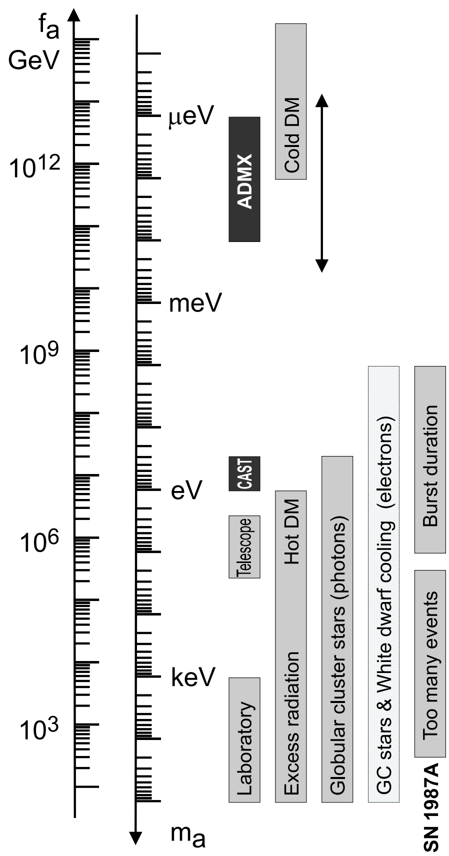

Figure 2: Exclusion and experimental search ranges as described in the text. Limits on coupling strengths are translated into limits on m_A and f_A using $z = 0.56$ and the KSVZ values for the coupling strengths. The "Laboratory" bar is a rough representation of the exclusion range for standard or variant axions. The "GC stars and white-dwarf cooling" range uses the DFSZ model with an axion-electron coupling corresponding to $\cos^2\beta = 1/2$. The Cold Dark Matter exclusion range is particularly uncertain. We show the benchmark case from the misalignment mechanism.

limit $\alpha_{Aee} \lesssim 1 \times 10^{-26}$ from the white-dwarf luminosity function [46]. For pulsationally unstable white dwarfs (ZZ Ceti stars), the period decrease $\dot{P}/P$ is a measure of the cooling speed. A well-studied case is the star G117–B15A, where $\dot{P}/P$ has been measured, implying [47]

$$\alpha_{Aee} < 1.3 \times 10^{-27} \tag{15}$$

at a statistical 95% CL. (We have corrected the published limit for an apparent misprint.) This result is equivalent to $g_{Aee} < 1.3 \times 10^{-13}$ or in the DFSZ model to $f_A > 1.3 \times 10^9$ GeV $\cos^2\beta$ and $m_A < 4.5$ meV$/\cos^2\beta$. We show these constraints in Figure 2 for $\cos^2\beta = 1/2$.

Similar constraints are provided by the neutrino signal of the supernova SN 1987A. Several detectors registered together about two dozen events spread over about 10 s, showing that the burst duration was not significantly shortened by a new energy-loss channel. Numerical simulations for a variety of cases, including axions and Kaluza-Klein gravitons, reveal that the energy-loss rate of a nuclear medium at the density 3×10^{14} g cm^{-3} and temperature 30 MeV should not exceed about 1×10^{19} erg g^{-1} s^{-1} [39]. Translating this nominal criterion into a limit on the axion-nucleon coupling depends on a calculation of bremsstrahlung emission $N + N \to N + N + a$ in a nuclear medium. The energy loss rate per unit mass is found to be $(C_N/2f_A)^2(T^4/\pi^2 m_N)\,F$. Here F is a numerical factor that represents an integral over the dynamical spin-density structure function, because axions couple to the nucleon spin and thus are essentially emitted by the fluctuating nuclear spins of the dense medium. In a dilute medium, F would have the interpretation of $\Gamma/2T$ with Γ a typical nucleon spin fluctuation rate. For realistic conditions, even after considerable effort, one is limited to a heuristic estimate leading to $F \approx 1$ [40].

The SN 1987A limits are of particular interest for hadronic axions where the bounds on α_{Aee} are moot. Therefore, we use $C_p = -0.4$ and $C_n = 0$. We use an initial proton fraction of 0.3 to scale the emission rate to the proton density. With $F = 1$ and $T = 30$ MeV we find [40]

$$f_A \gtrsim 4 \times 10^8 \text{ GeV} \qquad \text{and} \qquad m_A \lesssim 16 \text{ meV}\,. \tag{16}$$

If axions interact sufficiently strongly they are trapped, like neutrinos, so that only about three orders of magnitude in g_{ANN} or m_A are excluded by the burst duration. We show the excluded range somewhat schematically in Figure 2. For even larger couplings, the axion flux would have been negligible, yet it would have triggered additional events in the detectors, excluding a further range of couplings [48]. A possible gap between the exclusion ranges of these two SN 1987A arguments was discussed as the "hadronic axion window" under the assumption that $G_{A\gamma\gamma}$ was anomalously small [49]. This range is now excluded by the cosmic structure-formation arguments to be discussed in the section on cosmological axions.

III.2 Searches for solar axions: Instead of using stellar energy losses to derive limits on axion parameters, one can also search directly for these fluxes in the laboratory, notably those from our Sun. The main experimental focus has been on axion-like particles with a two-photon vertex. They are produced by the Primakoff process with a flux given by Equation 13, and can be detected at Earth with the reverse process in a macroscopic B–field ("axion helioscope") [22]. Viewing this re-conversion as a particle oscillation process, we note that the average energy of solar axions is 4.2 keV, implying a photon-axion oscillation length in vacuum of $2\pi\,(2\omega/m_A^2) \sim \mathcal{O}(1 \text{ mm})$, precluding the vacuum mixing from achieving its theoretical maximum in any practical magnet. However, one can endow the photon with an effective mass in a gas, $m_\gamma = \omega_{\text{plas}}$, thus matching the axion and photon dispersion relations [50].

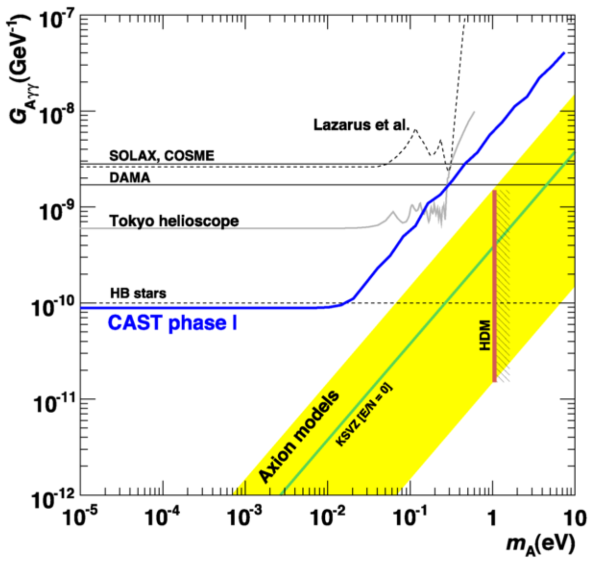

Figure 3: Solar-axion exclusion plot in the $G_{A\gamma\gamma}$–m_A–plane for axion-like particles [53]. For small masses, the most restrictive limit is from CAST-I [53], and is shown with previous helioscopes Lazarus *et al.* [51] and the Tokyo helioscope [52]. Also shown are constraints from experiments using the Bragg technique SOLAX [55], COSME [56], and DAMA [57]. The vertical red line (HDM) is the hot dark-matter limit [64]. The yellow band represents models with $|E/N - 1.92|$ in the range 0.07–7, while the green solid line corresponds to the KSVZ case.

An early implementation of these ideas was carried out using a conventional dipole magnet, with a conversion volume of variable-pressure gas with a xenon proportional chamber as x-ray detector [51]. The conversion magnet was fixed in orientation and collected data for about 1000 s/day. Axions were excluded for $G_{A\gamma\gamma} < 3.6 \times 10^{-9}$ GeV^{-1} for $m_A < 0.03$ eV, and $G_{A\gamma\gamma} < 7.7 \times 10^{-9}$ GeV^{-1} for $0.03 < m_A < 0.11$ eV at 95% CL. Later, the Tokyo axion helioscope used a superconducting magnet on a tracking mount, viewing the Sun continuously. They reported $G_{A\gamma\gamma} < 6 \times 10^{-10}$ GeV^{-1} for $m_A < 0.3$ eV [52]. The exclusion ranges are shown in Figure 3.

The most recent helioscope CAST (CERN Axion Solar Telescope) uses a decommissioned LHC dipole magnet on a tracking mount and is actively taking data. The hardware includes grazing-incidence x-ray optics with solid-state x-ray detectors, as well as a novel x-ray Micromegas position-sensitive gaseous detector. CAST has established a 95% CL limit $G_{A\gamma\gamma} < 8.8 \times 10^{-11}$ GeV^{-1} for $m_a < 0.02$ eV [53]. To cover larger masses and to "cross the axion line," the conversion region in the magnet bores is filled with a gas at varying pressure. The runs with ^{4}He gas are complete and cover masses up to about 0.4 eV, but exact limits on $G_{A\gamma\gamma}$ in this range have not yet been established [54]. Forthcoming runs with ^{3}He gas will explore axion masses up to 1.16 eV within about 3 years.

Other Primakoff searches for solar axions have been carried out using crystal detectors, exploiting the coherent conversion of axions into photons when the axion angle of incidence satisfies a Bragg condition with a crystalline plane. Limits from SOLAX [55], COSME [56], and DAMA [57] are summarized in Figure 4.

Another idea is to look at the Sun with an x-ray satellite when the Earth is in between. Solar axions would be converted in the Earth magnetic field on the far side relative to the Sun into x-rays, and could be picked up by the detector [58]. The sensitivity to $G_{A\gamma\gamma}$ could be comparable to CAST, but only for much smaller m_A.

III.3 Conversion of astrophysical photon fluxes: Large-scale magnetic fields exist in astrophysics that can induce axion–photon oscillations. In practical cases, B is much smaller than the laboratory fields used, for example, in helioscopes, whereas the conversion region L is much larger. Therefore, while the product BL can be large, any realistic sensitivity is usually restricted to very low-mass particles, far away from the "axion line" in a plot like Figure 3.

One example is SN 1987A, which would have emitted a burst of axion-like particles due to the Primakoff production in its core. They would have partially converted into γ-rays in the galactic B-field. The absence of a γ-ray burst in coincidence with the SN 1987A neutrino burst provides a limit $G_{A\gamma\gamma} \lesssim 1 \times 10^{-11}$ GeV^{-1} for $m_A \lesssim 10^{-9}$ eV [59]. This is the most restrictive limit for very small m_A.

Axion-like particles from other stars could be converted to photons in astrophysical B-fields, but no tangible new limits or signatures seem to have appeared.

Conversely, photons from distant sources could be converted to axion-like particles, depleting the original flux, thereby dimming the sources. This mechanism was proposed as an alternative explanation to cosmic acceleration for the apparent dimming of distant SNe of type Ia [60]. However, this dimming would apply to all distant sources, including quasars and the cosmic microwave background radiation, and would depend on energy. All things considered, this mechanism can only play a subdominant role [61].

High-energy γ-rays are typically produced in magnetized environments where cosmic rays are accelerated. The conversion into axion-like particles can then, in principle, imprint observable features on the spectrum for a range of coupling constants not excluded by other arguments [62].

IV. COSMIC AXIONS

IV.1 Cosmic axion populations: In the early universe, axions are produced by processes involving their couplings to quarks and gluons [63]. After the QCD confinement transition, the dominant thermalization process is $\pi + \pi \leftrightarrow \pi + a$ [21]. The resulting cosmic axion population would contribute a hot dark-matter fraction in analogy to massive neutrinos. Cosmological precision data provide restrictive constraints on a possible hot dark-matter fraction that translate into $m_A < 0.4$–1.2 eV at the 95% statistical CL [64]. The spread of the published limits reflects the use of different cosmological data. Including Lyman-α data leads to more restrictive limits that are, however, vulnerable to poorly controlled systematic uncertainties.

For $m_A \gtrsim 20$ eV, axions decay into photons faster than a cosmic time scale, removing the axion population while injecting radiation. This excess radiation provides additional limits up to very large axion masses [65]. An anomalously small $G_{A\gamma\gamma}$ provides no loophole because suppressing decays leads to thermal axions overdominating the mass density of the universe.

The main cosmological interest in axions derives from their possible role as cold dark matter (CDM). In addition to thermal processes, axions are abundantly produced by the "misalignment mechanism" [66]. After the spontaneous breakdown of the PQ symmetry at high energies, the axion field relaxes somewhere in the "bottom of the wine bottle" potential. Near the QCD epoch, instanton effects explicitly break the PQ symmetry, the very effect that causes the dynamical PQ symmetry restoration. This "tilting of the wine bottle bottom" causes the axion field to roll toward the CP-conserving minimum, thereby exciting coherent oscillations of the axion field that ultimately represent a "condensate" of CDM. The cosmic mass density in this homogeneous field mode is [67]

$$\Omega_A h^2 \approx 0.7 \left(\frac{f_A}{10^{12}\ \text{GeV}}\right)^{7/6} \left(\frac{\bar{\Theta}_\text{i}}{\pi}\right)^2 , \qquad (17)$$

where h is the present-day Hubble expansion parameter in units of 100 km s^{-1} Mpc^{-1}, and $-\pi \leq \bar{\Theta}_\text{i} \leq \pi$ is the initial "misalignment angle" relative to the CP-conserving position. If the PQ symmetry breakdown takes place after inflation, $\bar{\Theta}_\text{i}$ will take on different values in different patches of the universe. The average contribution is [67]

$$\Omega_A h^2 \approx 0.3 \left(\frac{f_A}{10^{12}\ \text{GeV}}\right)^{7/6} . \qquad (18)$$

Comparing with the measured CDM density of $\Omega_\text{CDM} h^2 \approx 0.13$ implies that axions with $m_A \approx 10$ μeV provide the dark matter, whereas smaller masses are excluded (Figure 2).

This density sets only a crude scale of the expected m_A. Apart from the overall particle physics uncertainties, the cosmological sequence of events plays a crucial role. Assuming axions make up CDM, significantly smaller masses are possible if inflation took place after the PQ transition and the initial value $\bar{\Theta}_\text{i}$ was small. Conversely, if the PQ transition took place after inflation, there are additional sources for nonthermal axions, notably the formation and decay of cosmic strings and domain walls. However, these populations are comparable to the misalignment contribution [67]. Still, the mass of CDM axions could be significantly smaller or larger than 10 μeV [67].

If the reheat temperature after inflation is too small to restore the PQ symmetry, the axion field is present during inflation, and subject to quantum mechanical fluctuations that lead to isocurvature fluctuations that are severely constrained by precision cosmological data [67,68]. One consequence is that the cosmic axion population cannot be arbitrarily small, even for a very small initial $\bar{\Theta}_\text{i}$.

In the opposite case without inflation after the PQ transition, the spatial axion density variation is large at the QCD transition. These density variations are not erased by free streaming. When matter begins to dominate the universe, gravitationally bound "axion mini clusters" form promptly [69]. A significant fraction of CDM axions can reside in these objects.

The hot and cold cosmic axion populations are not entirely independent. Most cold axions are produced shortly before the QCD phase transition. For $f_A \lesssim 10^8$ GeV, axions reach thermal equilibrium after this epoch, thermalizing the axion field, thereby erasing the cold populations.

IV.2 Telescope searches: The two-photon decay rate of cosmic axions is extremely slow for axions with masses in the CDM regime, but could be detectable for eV-mass axions. The signature would be a quasi-monochromatic emission line from galaxies and galaxy clusters. This line, corrected for the host Doppler shift, would appear at half the axion mass, and its width would be similar to the virial width of objects in the host. The expected optical line intensity for DFSZ axions is similar to the continuum night emission. An early search in three rich Abell clusters [70], and a recent search in two rich Abell clusters [71], exclude the "Telescope" range in Figure 2 unless the axion–photon coupling is strongly suppressed. Of course, axions in this mass range would also provide an excessive hot DM contribution.

Very low-mass axions in halos produce a weak quasi-monochromatic spectral line in the radio. Virial velocities in undisrupted dwarf galaxies are very low, and the axion emission line would therefore be extremely narrow. A search with the Haystack radio telescope on three nearby dwarf galaxies provided a limit $G_{A\gamma\gamma} < 1.0 \times 10^{-9}$ GeV^{-1} at 96% CL for $298 < m_A < 363$ μeV [72]. However, this combination of m_A and $G_{A\gamma\gamma}$ does not yet include plausible axion models.

IV.3 Microwave cavity experiments: The astrophysical and cosmological limits of Figure 2 suggest that axions, if they exist, provide a significant fraction or all of the cosmic CDM. In a broad range of the plausible m_A range for CDM axions, galactic halo axions may be detected by their resonant conversion into a quasi-monochromatic microwave signal in a high-Q electromagnetic cavity permeated by a strong static magnetic field [22,73]. The cavity frequency is tunable, and the signal is maximized when the frequency is the total axion energy, rest mass plus kinetic energy, of $\nu = (m_A/2\pi)\,[1 + \mathcal{O}(10^{-6})]$, the width above the rest mass representing the virial axion distribution in the galactic gravitational potential. The frequency spectrum width may also have finer structure from axions more recently fallen into the galactic potential and not yet completely virialized [74].

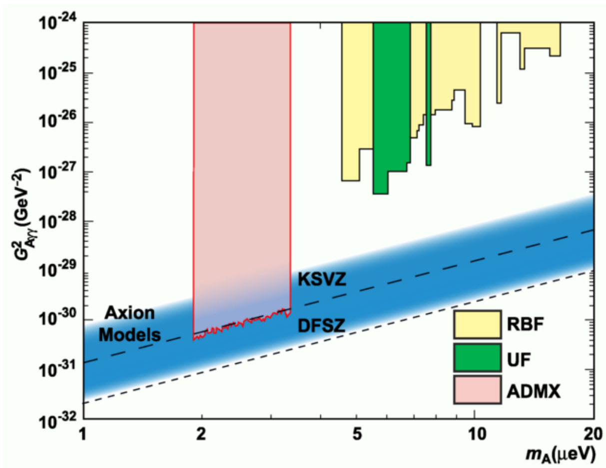

Figure 4: Exclusion region reported from the microwave cavity experiments RBF and UF [75] and ADMX [76]. A local dark-matter density of 450 MeV cm^{-3} is assumed. Color version at end of book.

The feasibility of this technique was established in early experiments of relatively small sensitive volume, $\mathcal{O}$(1 liter) [75], with HFET-based amplifiers, setting limits in the range $4.5 < m_A < 16.3$ μeV, but lacking by 2–3 orders of magnitude the sensitivity required to detect realistic axions. ADMX, a later experiment ($B \sim 8$ T, $V \sim 200$ liters) has achieved sensitivity to KSVZ axions, assuming they saturate the local dark matter halo and are well virialized, over the mass range 1.9–3.3 μeV [76]. Should halo axions have a component not yet virialized, ADMX is sensitive to DFSZ axions [77]. The corresponding 90% CL exclusion regions shown in Figure 4 are normalized to an assumed local CDM density of 7.5×10^{-25} g cm^{-3} (450 MeV cm^{-3}) [78]. The ADMX experiment is currently undergoing commissioning of an upgrade that replaces the microwave HFET amplifiers by near quantum-limited low-noise dc SQUID amplifiers [79], allowing a significant improvement in the experiment sensitivity. A Rydberg atom single-photon detector [80] can in principle evade the standard quantum limit [81] for coherent detection, thus achieving very good sensitivity. Efforts are underway to incorporate Rydberg atom systems in RF cavity axion searches [82].

Conclusions: Experimental, astrophysical, and cosmological limits have been refined and indicate that axions, if they exist, are likely very light, $m_A \lesssim 10$ meV, suggesting that axions are a non-negligible fraction of the cosmic CDM. The upgraded versions of the ADMX experiment will ultimately cover the range 1–100 μeV with a sensitivity allowing one to detect axions, unless the local DM density is unexpectedly small or the axion–photon coupling anomalously weak. Other experimental techniques remain of interest to search for general axion-like particles, although at present no method besides the DM search is known that could detect realistic axions obeying the astrophysical and cosmological limits, and fulfilling the QCD-implied relationship between mass and coupling strength.

References

1. R.D. Peccei and H. Quinn, Phys. Rev. Lett. **38**, 1440 (1977), Phys. Rev. **D16**, 1791 (1977).
2. S. Weinberg, Phys. Rev. Lett. **40**, 223 (1978);
   F. Wilczek, Phys. Rev. Lett. **40**, 279 (1978).
3. F. Wilczek, Phys. Rev. Lett. **49**, 1549 (1982).
4. Y. Chikashige, R.N. Mohapatra, and R.D. Peccei, Phys. Lett. **98B**, 265 (1981);
   G.B. Gelmini and M. Roncadelli, Phys. Lett. **99B**, 411 (1981).
5. C.A. Baker *et al.*, Phys. Rev. Lett. **97**, 131801 (2006).
6. H. Georgi, D.B. Kaplan, and L. Randall, Phys. Lett. **B169**, 73 (1986).
7. H. Leutwyler, Phys. Lett. **B378**, 313 (1996).
8. W.M. Yao *et al.*, (Particle Data Group), J. Phys. G: Nucl. Part. Phys. **33**, 1 (2006).
9. T.W. Donnelly *et al.*, Phys. Rev. **D18**, 1607 (1978);
   S. Barshay *et al.*, Phys. Rev. Lett. **46**, 1361 (1981);
   A. Barroso and N.C. Mukhopadhyay, Phys. Lett. **B106**, 91 (1981);
   R.D. Peccei, in *Proceedings of Neutrino '81*, Honolulu, Hawaii, Vol. 1, p. 149 (1981);
   L.M. Krauss and F. Wilczek, Phys. Lett. **B173**, 189 (1986).
10. J. Schweppe *et al.*, Phys. Rev. Lett. **51**, 2261 (1983);
    T. Cowan *et al.*, Phys. Rev. Lett. **54**, 1761 (1985).
11. R.D. Peccei, T.T. Wu, and T. Yanagida, Phys. Lett. **B172**, 435 (1986).
12. W.A. Bardeen, R.D. Peccei, and T. Yanagida, Nucl. Phys. **B279**, 401 (1987).
13. J.E. Kim, Phys. Rev. Lett. **43**, 103 (1979);
    M.A. Shifman, A.I. Vainstein, and V.I. Zakharov, Nucl. Phys. **B166**, 493 (1980).
14. M. Dine, W. Fischler, and M. Srednicki, Phys. Lett. **B104**, 199 (1981);
    A.R. Zhitnitsky, Sov. J. Nucl. Phys. **31**, 260 (1980).
15. K.S. Choi, I.W. Kim, and J.E. Kim, JHEP **0703**, 116 (2007).
16. S.L. Cheng, C.Q. Geng, and W.T. Ni, Phys. Rev. **D52**, 3132 (1995).
17. G. Raffelt and D. Seckel, Phys. Rev. Lett. **60**, 1793 (1988);
    M. Carena and R.D. Peccei, Phys. Rev. **D40**, 652 (1989);
    K. Choi, K. Kang, and J.E. Kim, Phys. Rev. Lett. **62**, 849 (1989).
18. V.Y. Alexakhin *et al.*, (COMPASS Collaboration), Phys. Lett. **B647**, 8 (2007).
19. A. Airapetian *et al.*, (HERMES Collaboration), Phys. Rev. **D75**, 012007 (2007) and Erratum *ibid.*, **D76**, 039901 (2007).
20. J.R. Ellis and M. Karliner, in: *The spin structure of the nucleon: International school of nucleon structure* (3–10 August 1995, Erice, Italy), ed. by B. Frois, V.W. Hughes, and N. De Groot (World Scientific, Singapore, 1997) `[hep-ph/9601280]`.
21. S. Chang and K. Choi, Phys. Lett. **B316**, 51 (1993).

22. P. Sikivie, Phys. Rev. Lett. **51**, 1415 (1983) and Erratum *ibid.*, **52**, 695 (1984).
23. D.A. Dicus *et al.*, Phys. Rev. **D18**, 1829 (1978).
24. G. Raffelt and L. Stodolsky, Phys. Rev. **D37**, 1237 (1988).
25. K. van Bibber *et al.*, Phys. Rev. Lett. **59**, 759 (1987).
26. G. Ruoso *et al.*, Z. Phys. **C56**, 505 (1992);
R. Cameron *et al.*, Phys. Rev. **D47**, 3707 (1993).
27. A. Afanasev *et al.*, arXiv:hep-ph/0605250.
28. C. Robilliard *et al.*, Phys. Rev. Lett. **99**, 190403 (2007).
29. A.S. Chou *et al.* (GammeV Collab.), Phys. Rev. Lett. **100**, 080402 (2008).
30. P. Sikivie, D. Tanner, and K. van Bibber, Phys. Rev. Lett. **98**, 172002 (2007).
31. L. Maiani *et al.*, Phys. Lett. **B175**, 359 (1986).
32. Y. Semertzidis *et al.*, Phys. Rev. Lett. **64**, 2988 (1990).
33. E. Zavattini *et al.*, (PVLAS Collab.), Phys. Rev. Lett. **96**, 110406 (2006).
34. E. Zavattini *et al.*, (PVLAS Collab.), Phys. Rev. **D77**, 032006 (2008).
35. E. Fischbach and C. Talmadge, Nature **356**, 207 (1992).
36. J.E. Moody and F. Wilczek, Phys. Rev. D 30, 130(1984).
37. A.N. Youdin *et al.*, Phys. Rev. Lett. **77**, 2170 (1996);
Wei-Tou Ni *et al.*, Phys. Rev. Lett. **82**, 2439 (1999);
D.F. Phillips *et al.*, Phys. Rev. **D63**, 111101 (R)(2001);
B.R. Heckel *et al.*, (Eöt-Wash Collaboration), Phys. Rev. Lett. **97**, 021603 (2006).
38. M.S. Turner, Phys. Reports **197**, 67 (1990);
G.G. Raffelt, Phys. Reports **198**, 1 (1990).
39. G.G. Raffelt, *Stars as Laboratories for Fundamental Physics*, (Univ. of Chicago Press, Chicago, 1996).
40. G.G. Raffelt, Lect. Notes Phys. **741**, 51 (2008) (Springer Verlag).
41. H. Schlattl, A. Weiss, and G. Raffelt, Astropart. Phys. **10**, 353 (1999).
42. J.N. Bahcall, A.M. Serenelli, and S. Basu, Astrophys. J. **21**, L85 (2005).
43. Q.R. Ahmad *et al.*, (SNO Collaboration), Phys. Rev. Lett. **89**, 011301 (2002);
B. Aharmim *et al.*, (SNO Collaboration), Phys. Rev. **C72**, 055502 (2005).
44. A. Buzzoni *et al.*, Astron. Astrophys. **128**, 94 (1983).
45. G. Raffelt and A. Weiss, Phys. Rev. **D51**, 1495 (1995);
M. Catelan, J.A. de Freitas Pacheco, and J.E. Horvath, Astrophys. J. **461**, 231 (1996).
46. G.G. Raffelt, Phys. Lett. **B166**, 402 (1986);
S.I. Blinnikov and N.V. Dunina-Barkovskaya, Mon. Not. R. Astron. Soc. **266**, 289 (1994).
47. A.H. Córsico *et al.*, New Astron. **6**, 197 (2001);
J. Isern and E. García-Berro, Nucl. Phys. B Proc. Suppl. **114**, 107 (2003).
48. J. Engel, D. Seckel, and A.C. Hayes, Phys. Rev. Lett. **65**, 960 (1990).
49. T. Moroi and H. Murayama, Phys. Lett. **B440**, 69 (1998).
50. K. van Bibber *et al.*, Phys. Rev. **D39**, 2089 (1989).
51. D. Lazarus *et al.*, Phys. Rev. Lett. **69**, 2333 (1992).
52. S. Moriyama *et al.*, Phys. Lett. **B434**, 147 (1998);
Y. Inoue *et al.*, Phys. Lett. **B536**, 18 (2002).
53. K. Zioutas *et al.*, (CAST Collaboration), Phys. Rev. Lett. **94**, 121301 (2005);
S. Andriamonje *et al.*, (CAST Collaboration), JCAP **0704**, 010 (2007).
54. K. Zioutas *et al.*, (CAST Collaboration), "Status Report of the CAST experiment and request to run beyond 2007," CERN-SPSC-2007-013 (5 April 2007), see http://doc.cern.ch//archive/electronic/cern/preprints/spsc/public/spsc-2007-013.pdf.
55. F.T. Avignone III *et al.*, Phys. Rev. Lett. **81**, 5068 (1998).
56. A. Morales *et al.*, (COSME Collaboration), Astropart. Phys. **16**, 325 (2002).
57. R. Bernabei *et al.*, Phys. Lett. **B515**, 6 (2001).
58. H. Davoudiasl and P. Huber, Phys. Rev. Lett. **97**, 141302 (2006).
59. J.W. Brockway, E.D. Carlson, and G.G. Raffelt, Phys. Lett. **B383**, 439 (1996);
J.A. Grifols, E.Massó, and R. Toldrà, Phys. Rev. Lett. **77**, 2372 (1996).
60. C. Csaki, N. Kaloper, and J. Terning, Phys. Rev. Lett. **88**, 161302 (2002).
61. A. Mirizzi, G.G. Raffelt, and P.D. Serpico, Lect. Notes Phys. **741**, 115 (2008).
62. D. Hooper and P.D. Serpico, Phys. Rev. Lett. **99**, 231102 (2007);
K.A. Hochmuth and G. Sigl, Phys. Rev. **D76**, 123011 (2007).
63. M.S. Turner, Phys. Rev. Lett. **59**, 2489 (1987) and Erratum *ibid.*, **60**, 1101 (1988);
E. Massó, F. Rota, and G. Zsembinszki, Phys. Rev. **D66**, 023004 (2002).
64. S. Hannestad, A. Mirizzi, and G. Raffelt, JCAP **0507**, 002 (2005);
A. Melchiorri, O. Mena, and A. Slosar, Phys. Rev. **D76**, 041303 (2007);
S. Hannestad *et al.*, JCAP **0708**, 015 (2007).
65. E. Massó and R. Toldra, Phys. Rev. **D55**, 7967 (1997).
66. J. Preskill, M.B. Wise, and F. Wilczek, Phys. Lett. **B120**, 127 (1983);
L.F. Abbott and P. Sikivie, Phys. Lett. **B120**, 133 (1983);
M. Dine and W. Fischler, Phys. Lett. **B120**, 137 (1983).
67. P. Sikivie, Lect. Notes Phys. **741**, 19 (2008).
68. M. Beltrán, J. García-Bellido, and J. Lesgourgues, Phys. Rev. **D75**, 103507 (2007).
69. E.W. Kolb and I.I. Tkachev, Phys. Rev. Lett. **71**, 3051 (1993);
E.W. Kolb and I.I. Tkachev, Astrophys. J. **460**, L25 (1996).
70. M. Bershady *et al.*, Phys. Rev. Lett. **66**, 1398 (1991);
M. Ressell, Phys. Rev. **D44**, 3001 (1991).
71. D. Grin *et al.*, Phys. Rev. **D5**, 105018 (2007).
72. B.D. Blout *et al.*, Astrophys. J. **546**, 825 (2001).
73. P. Sikivie, Phys. Rev. **D32**, 2988 (1985);
L. Krauss *et al.*, Phys. Rev. Lett. **55**, 1797 (1985);
R. Bradley *et al.*, Rev. Mod. Phys. **75**, 777 (2003).
74. P. Sikivie and J. Ipser, Phys. Lett. **B291**, 288 (1992);
P. Sikivie *et al.*, Phys. Rev. Lett. **75**, 2911 (1995).
75. S. DePanfilis *et al.*, Phys. Rev. Lett. **59**, 839 (1987);
W. Wuensch *et al.*, Phys. Rev. **D40**, 3153 (1989);
C. Hagmann *et al.*, Phys. Rev. **D42**, 1297 (1990).
76. S. Asztalos *et al.*, Phys. Rev. **D69**, 011101 (2004).
77. L. Duffy *et al.*, Phys. Rev. Lett. **95**, 091304 (2005).

78. E. Gates *et al.*, Astrophys. J. **449**, 123 (1995).
79. M. Mück, J.B. Kycia, and J. Clarke, Appl. Phys. Lett. **78**, 967 (2001).
80. I. Ogawa, S. Matsuki, and K. Yamamoto, Phys. Rev. **D53**, 1740 (1996).
81. V. Braginsky and F. Khalili in: *Quantum Measurement*, ed. by K. Thorne (Cambridge University Press, Cambridge) 1992.
82. S. Matsuki *et al.*, Nucl. Phys. B (Proc. Suppl.) **51**, 213 (1996);
Y. Kishimoto *et al.*, Phys. Lett. **A303**, 279 (2002);
M. Tada *et al.*, Phys. Lett. **A303**, 285 (2002).

A^0 (Axion) MASS LIMITS from Astrophysics and Cosmology

These bounds depend on model-dependent assumptions (i.e. — on a combination of axion parameters).

VALUE (MeV)	*DOCUMENT ID*		*TECN*	*COMMENT*
• • • We do not use the following data for averages, fits, limits, etc. • • •				
>0.2	BARROSO	82	ASTR	Standard Axion
>0.25	[1] RAFFELT	82	ASTR	Standard Axion
>0.2	[2] DICUS	78C	ASTR	Standard Axion
	MIKAELIAN	78	ASTR	Stellar emission
>0.3	[2] SATO	78	ASTR	Standard Axion
>0.2	VYSOTSKII	78	ASTR	Standard Axion

[1] Lower bound from 5.5 MeV γ-ray line from the sun.
[2] Lower bound from requiring the red giants' stellar evolution not be disrupted by axion emission.

A^0 (Axion) and Other Light Boson (X^0) Searches in Hadron Decays

Limits are for branching ratios.

VALUE	*CL%*	*DOCUMENT ID*		*TECN*	*COMMENT*
• • • We do not use the following data for averages, fits, limits, etc. • • •					
		[3] PARK	05	HYCP	$\Sigma^+ \to pA^0$, $A^0 \to \mu^+\mu^-$
$<7 \times 10^{-10}$	90	[4] ADLER	04	B787	$K^+ \to \pi^+ X^0$
$<7.3 \times 10^{-11}$	90	[5] ANISIMOVSK...	04	B949	$K^+ \to \pi^+ X^0$
$<4.5 \times 10^{-11}$	90	[6] ADLER	02C	B787	$K^+ \to \pi^+ X^0$
$<4 \times 10^{-5}$	90	[7] ADLER	01	B787	$K^+ \to \pi^+\pi^0 A^0$
$<4.9 \times 10^{-5}$	90	AMMAR	01B	CLEO	$B^\pm \to \pi^\pm(K^\pm)X^0$
$<5.3 \times 10^{-5}$	90	AMMAR	01B	CLEO	$B^0 \to K^0_S X^0$
$<3.3 \times 10^{-5}$	90	[8] ALTEGOER	98	NOMD	$\pi^0 \to \gamma X^0$, $m_{X^0} < 120$ MeV
$<5.0 \times 10^{-8}$	90	[9] KITCHING	97	B787	$K^+ \to \pi^+ X^0$ $(X^0 \to \gamma\gamma)$
$<5.2 \times 10^{-10}$	90	[10] ADLER	96	B787	$K^+ \to \pi^+ X^0$
$<2.8 \times 10^{-4}$	90	[11] AMSLER	96B	CBAR	$\pi^0 \to \gamma X^0$, $m_{X^0} < 65$ MeV
$<3 \times 10^{-4}$	90	[11] AMSLER	96B	CBAR	$\eta \to \gamma X^0$, m_{X^0}= 50–200 MeV
$<4 \times 10^{-5}$	90	[11] AMSLER	96B	CBAR	$\eta' \to \gamma X^0$, m_{X^0}= 50–925 MeV
$<6 \times 10^{-5}$	90	[11] AMSLER	94B	CBAR	$\pi^0 \to \gamma X^0$, m_{X^0}=65–125 MeV
$<6 \times 10^{-5}$	90	[11] AMSLER	94B	CBAR	$\eta \to \gamma X^0$, m_{X^0}=200–525 MeV
$<7 \times 10^{-3}$	90	[12] MEIJERDREES	94	CNTR	$\pi^0 \to \gamma X^0$, m_{X^0}=25 MeV
$<2 \times 10^{-3}$	90	[12] MEIJERDREES	94	CNTR	$\pi^0 \to \gamma X^0$, m_{X^0}=100 MeV
$<2 \times 10^{-7}$	90	[13] ATIYA	93B	B787	Sup. by ADLER 04
$<3 \times 10^{-13}$		[14] NG	93	COSM	$\pi^0 \to \gamma X^0$
$<1.1 \times 10^{-8}$	90	[15] ALLIEGRO	92	SPEC	$K^+ \to \pi^+ X^0$ $(X^0 \to e^+e^-)$
$<5 \times 10^{-4}$	90	[16] ATIYA	92	B787	$\pi^0 \to \gamma X^0$
$<4 \times 10^{-6}$	90	[17] MEIJERDREES	92	SPEC	$\pi^0 \to \gamma X^0$, $X^0 \to e^+e^-$, m_{X^0}= 100 MeV
$<1 \times 10^{-7}$	90	[18] ATIYA	90B	B787	Sup. by KITCHING 97
$<1.3 \times 10^{-8}$	90	[19] KORENCHE...	87	SPEC	$\pi^+ \to e^+\nu A^0$ $(A^0 \to e^+e^-)$
$<1 \times 10^{-9}$	90	[20] EICHLER	86	SPEC	Stopped $\pi^+ \to e^+\nu A^0$
$<2 \times 10^{-5}$	90	[21] YAMAZAKI	84	SPEC	For 160<m<260 MeV
$<(1.5–4) \times 10^{-6}$	90	[21] YAMAZAKI	84	SPEC	K decay, $m_{X^0} \ll 100$ MeV
		[22] ASANO	82	CNTR	Stopped $K^+ \to \pi^+ X^0$
		[23] ASANO	81B	CNTR	Stopped $K^+ \to \pi^+ X^0$
		[24] ZHITNITSKII	79		Heavy axion

[3] PARK 05 found three candidate events for $\Sigma^+ \to p\mu^+\mu^-$ in the HyperCP experiment. Due to a narrow spread in dimuon mass, they hypothesize the events as a possible signal of a new boson. It can be interpreted as an axion-like particle with m_{A^0} = 214.3 ± 0.5 MeV and the branching fraction $B(\Sigma^+ \to pA^0)\times B(A^0 \to \mu^+\mu^-) = (3.1^{+2.4}_{-1.9} \pm 1.5) \times 10^{-8}$.
[4] This limit applies for a mass near 180 MeV. For other masses in the range m_{X^0} = 150–250 MeV the limit is less restrictive, but still improves ADLER 02C and ATIYA 93B.
[5] ANISIMOVSKY 04 bound is for m_{X^0}=0.
[6] ADLER 02C bound is for m_{X^0} <60 MeV. See Fig. 2 for limits at higher masses.
[7] The quoted limit is for m_{X^0} = 0–80 MeV. See their Fig. 5 for the limit at higher mass. The branching fraction limit assumes pure phase space decay distributions.
[8] ALTEGOER 98 looked for X^0 from π^0 decay which penetrate the shielding and convert to π^0 in the external Coulomb field of a nucleus.
[9] KITCHING 97 limit is for $B(K^+ \to \pi^+ X^0)\cdot B(X^0 \to \gamma\gamma)$ and applies for $m_{X^0} \simeq 50$ MeV, $\tau_{X^0} < 10^{-10}$ s. Limits are provided for 0<m_{X^0} < 100 MeV, $\tau_{X^0} < 10^{-8}$ s.
[10] ADLER 96 looked for a peak in missing-mass distribution. This work is an update of ATIYA 93. The limit is for massless stable X^0 particles and extends to m_{X^0}=80 MeV at the same level. See paper for dependence on finite lifetime.
[11] AMSLER 94B and AMSLER 96B looked for a peak in missing-mass distribution.
[12] The MEIJERDREES 94 limit is based on inclusive photon spectrum and is independent of X^0 decay modes. It applies to $\tau(X^0) > 10^{-23}$ sec.
[13] ATIYA 93B looked for a peak in missing mass distribution. The bound applies for stable X^0 of m_{X^0}=150–250 MeV, and the limit becomes stronger (10^{-8}) for m_{X^0}=180–240 MeV.
[14] NG 93 studied the production of X^0 via $\gamma\gamma \to \pi^0 \to \gamma X^0$ in the early universe at $T \simeq 1$ MeV. The bound on extra neutrinos from nucleosynthesis $\Delta N_\nu < 0.3$ (WALKER 91) is employed. It applies to $m_{X^0} \ll 1$ MeV in order to be relativistic down to nucleosynthesis temperature. See paper for heavier X^0.
[15] ALLIEGRO 92 limit applies for m_{X^0}=150–340 MeV and is the branching ratio times the decay probability. Limit is $< 1.5 \times 10^{-8}$ at 99%CL.
[16] ATIYA 92 looked for a peak in missing mass distribution. The limit applies to m_{X^0}=0–130 MeV in the narrow resonance limit. See paper for the dependence on lifetime. Covariance requires X^0 to be a vector particle.
[17] MEIJERDREES 92 limit applies for $\tau_{X^0} = 10^{-23}$–10^{-11} sec. Limits between 2×10^{-4} and 4×10^{-6} are obtained for m_{X^0} = 25–120 MeV. Angular momentum conservation requires that X^0 has spin ≥ 1.
[18] ATIYA 90B limit is for $B(K^+ \to \pi^+ X^0)\cdot B(X^0 \to \gamma\gamma)$ and applies for m_{X^0} = 50 MeV, $\tau_{X^0} < 10^{-10}$ s. Limits are also provided for $0 < m_{X^0} < 100$ MeV, $\tau_{X^0} < 10^{-8}$ s.
[19] KORENCHENKO 87 limit assumes m_{A^0} = 1.7 MeV, $\tau_{A^0} \lesssim 10^{-12}$ s, and $B(A^0 \to e^+e^-) = 1$.
[20] EICHLER 86 looked for $\pi^+ \to e^+\nu A^0$ followed by $A^0 \to e^+e^-$. Limits on the branching fraction depend on the mass and and lifetime of A^0. The quoted limits are valid when $\tau(A^0) \gtrsim 3. \times 10^{-10}$s if the decays are kinematically allowed.
[21] YAMAZAKI 84 looked for a discrete line in $K^+ \to \pi^+ X$. Sensitive to wide mass range (5–300 MeV), independent of whether X decays promptly or not.
[22] ASANO 82 at KEK set limits for $B(K^+ \to \pi^+ X^0)$ for m_{X^0} <100 MeV as BR $< 4. \times 10^{-8}$ for $\tau(X^0 \to n\gamma\text{'s}) > 1. \times 10^{-9}$ s, BR $< 1.4 \times 10^{-6}$ for $\tau < 1. \times 10^{-9}$s.
[23] ASANO 81B is KEK experiment. Set $B(K^+ \to \pi^+ X^0) < 3.8 \times 10^{-8}$ at CL = 90%.
[24] ZHITNITSKII 79 argue that a heavy axion predicted by YANG 78 (3 <m <40 MeV) contradicts experimental muon anomalous magnetic moments.

A^0 (Axion) Searches in Quarkonium Decays

Decay or transition of quarkonium. Limits are for branching ratio.

VALUE	*CL%*	*DOCUMENT ID*		*TECN*	*COMMENT*
• • • We do not use the following data for averages, fits, limits, etc. • • •					
$<1.3 \times 10^{-5}$	90	[25] BALEST	95	CLEO	$\Upsilon(1S) \to A^0\gamma$
$<4.0 \times 10^{-5}$	90	ANTREASYAN	90C	CBAL	$\Upsilon(1S) \to A^0\gamma$
		[26] ANTREASYAN	90C	RVUE	
$<5 \times 10^{-5}$	90	[27] DRUZHININ	87	ND	$\phi \to A^0\gamma$ $(A^0 \to e^+e^-)$
$<2 \times 10^{-3}$	90	[28] DRUZHININ	87	ND	$\phi \to A^0\gamma$ $(A^0 \to \gamma\gamma)$
$<7 \times 10^{-6}$	90	[29] DRUZHININ	87	ND	$\phi \to A^0\gamma$ $(A^0 \to$ missing)
$<3.1 \times 10^{-4}$	90	[30] ALBRECHT	86D	ARG	$\Upsilon(1S) \to A^0\gamma$ $(A^0 \to e^+e^-)$
$<4 \times 10^{-4}$	90	[30] ALBRECHT	86D	ARG	$\Upsilon(1S) \to A^0\gamma$ $(A^0 \to \mu^+\mu^-$, $\pi^+\pi^-$, $K^+K^-)$
$<8 \times 10^{-4}$	90	[31] ALBRECHT	86D	ARG	$\Upsilon(1S) \to A^0\gamma$
$<1.3 \times 10^{-3}$	90	[32] ALBRECHT	86D	ARG	$\Upsilon(1S) \to A^0\gamma$ $(A^0 \to e^+e^-$, $\gamma\gamma)$
$<2. \times 10^{-3}$	90	[33] BOWCOCK	86	CLEO	$\Upsilon(2S) \to \Upsilon(1S) \to A^0$
$<5. \times 10^{-3}$	90	[34] MAGERAS	86	CUSB	$\Upsilon(1S) \to A^0\gamma$
$<3. \times 10^{-4}$	90	[35] ALAM	83	CLEO	$\Upsilon(1S) \to A^0\gamma$
$<9.1 \times 10^{-4}$	90	[36] NICZYPORUK	83	LENA	$\Upsilon(1S) \to A^0\gamma$
$<1.4 \times 10^{-5}$	90	[37] EDWARDS	82	CBAL	$J/\psi \to A^0\gamma$
$<3.5 \times 10^{-4}$	90	[38] SIVERTZ	82	CUSB	$\Upsilon(1S) \to A^0\gamma$
$<1.2 \times 10^{-4}$	90	[38] SIVERTZ	82	CUSB	$\Upsilon(3S) \to A^0\gamma$

[25] BALEST 95 looked for a monochromatic γ from $\Upsilon(1S)$ decay. The bound is for m_{A^0} < 5.0 GeV. See Fig. 7 in the paper for bounds for heavier m_{A^0}. They also quote a bound on branching ratios 10^{-3}–10^{-5} of three-body decay γXX for 0<m_X < 3.1 GeV.
[26] The combined limit of ANTREASYAN 90C and EDWARDS 82 excludes standard axion with $m_{A^0} < 2m_e$ at 90% CL as long as $C_\Upsilon C_{J/\psi} > 0.09$, where C_V $(V = \Upsilon, J/\psi)$ is the reduction factor for $\Gamma(V \to A^0\gamma)$ due to QCD and/or relativistic corrections. The same data excludes 0.02 $< x <$ 260 (90% CL) if $C_\Upsilon = C_{J/\psi}$ = 0.5, and further combining with ALBRECHT 86D result excludes $5 \times 10^{-5} < x < 260$. x is the ratio of the vacuum expectation values of the two Higgs fields. These limits use conventional assumption $\Gamma(A^0 \to ee) \propto x^{-2}$. The alternative assumption $\Gamma(A^0 \to ee) \propto x^2$ gives a somewhat different excluded region 0.00075 $< x <$ 44.
[27] The first DRUZHININ 87 limit is valid when $\tau_{A^0}/m_{A^0} < 3 \times 10^{-13}$ s/MeV and m_{A^0} < 20 MeV.
[28] The second DRUZHININ 87 limit is valid when $\tau_{A^0}/m_{A^0} < 5 \times 10^{-13}$ s/MeV and m_{A^0} < 20 MeV.
[29] The third DRUZHININ 87 limit is valid when $\tau_{A^0}/m_{A^0} > 7 \times 10^{-12}$ s/MeV and m_{A^0} < 200 MeV.

[30] $\tau_{A^0} < 1 \times 10^{-13}$s and $m_{A^0} < 1.5$ GeV. Applies for $A^0 \to \gamma\gamma$ when $m_{A^0} < 100$ MeV.
[31] $\tau_{A^0} > 1 \times 10^{-7}$s.
[32] Independent of τ_{A^0}.
[33] BOWCOCK 86 looked for A^0 that decays into e^+e^- in the cascade decay $\Upsilon(2S) \to \Upsilon(1S)\pi^+\pi^-$ followed by $\Upsilon(1S) \to A^0\gamma$. The limit for B($\Upsilon(1S) \to A^0\gamma$)B($A^0 \to e^+e^-$) depends on m_{A^0} and τ_{A^0}. The quoted limit for m_{A^0}=1.8 MeV is at $\tau_{A^0} \sim 2. \times 10^{-12}$s, where the limit is the worst. The same limit $2. \times 10^{-3}$ applies for all lifetimes for masses $2m_e < m_{A^0} < 2m_\mu$ when the results of this experiment are combined with the results of ALAM 83.
[34] MAGERAS 86 looked for $\Upsilon(1S) \to \gamma A^0$ ($A^0 \to e^+e^-$). The quoted branching fraction limit is for $m_{A^0} = 1.7$ MeV, at $\tau(A^0) \sim 4. \times 10^{-13}$s where the limit is the worst.
[35] ALAM 83 is at CESR. This limit combined with limit for B($J/\psi \to A^0\gamma$) (EDWARDS 82) excludes standard axion.
[36] NICZYPORUK 83 is DESY-DORIS experiment. This limit together with lower limit 9.2×10^{-4} of B($\Upsilon \to A^0\gamma$) derived from B($J/\psi(1S) \to A^0\gamma$) limit (EDWARDS 82) excludes standard axion.
[37] EDWARDS 82 looked for $J/\psi \to \gamma A^0$ decays by looking for events with a single γ [of energy $\sim 1/2$ the $J/\psi(1S)$ mass], plus nothing else in the detector. The limit is inconsistent with the axion interpretation of the FAISSNER 81B result.
[38] SIVERTZ 82 is CESR experiment. Looked for $\Upsilon \to \gamma A^0$, A^0 undetected. Limit for 1S (3S) is valid for m_{A^0} <7 GeV (4 GeV).

A^0 (Axion) Searches in Positronium Decays

Decay or transition of positronium. Limits are for branching ratio.

VALUE	CL%	DOCUMENT ID		TECN	COMMENT
• • • We do not use the following data for averages, fits, limits, etc. • • •					
$<4.4 \times 10^{-5}$	90	[39] BADERT...	02	CNTR	o-Ps $\to \gamma X_1 X_2$, $m_{X_1}+m_{X_2} \leq$ 900 keV
$<2 \times 10^{-4}$	90	MAENO	95	CNTR	o-Ps $\to A^0\gamma$ m_{A^0}=850–1013 keV
$<3.0 \times 10^{-3}$	90	[40] ASAI	94	CNTR	o-Ps $\to A^0\gamma$ m_{A^0}=30–500 keV
$<2.8 \times 10^{-5}$	90	[41] AKOPYAN	91	CNTR	o-Ps $\to A^0\gamma$ ($A^0 \to \gamma\gamma$), m_{A^0} < 30 keV
$<1.1 \times 10^{-6}$	90	[42] ASAI	91	CNTR	o-Ps $\to A^0\gamma$, m_{A^0} < 800 keV
$<3.8 \times 10^{-4}$	90	GNINENKO	90	CNTR	o-Ps $\to A^0\gamma$, m_{A^0} < 30 keV
$<(1–5) \times 10^{-4}$	95	[43] TSUCHIAKI	90	CNTR	o-Ps $\to A^0\gamma$, m_{A^0} = 300–900 keV
$<6.4 \times 10^{-5}$	90	[44] ORITO	89	CNTR	o-Ps $\to A^0\gamma$, m_{A^0} < 30 keV
		[45] AMALDI	85	CNTR	Ortho-positronium
		[46] CARBONI	83	CNTR	Ortho-positronium

[39] BADERTSCHER 02 looked for a three-body decay of ortho-positronium into a photon and two penetrating (neutral or milli-charged) particles.
[40] The ASAI 94 limit is based on inclusive photon spectrum and is independent of A^0 decay modes.
[41] The AKOPYAN 91 limit applies for a short-lived A^0 with $\tau_{A^0} < 10^{-13}$ m_{A^0} [keV] s.
[42] ASAI 91 limit translates to $g^2_{A^0 e^+ e^-}/4\pi < 1.1 \times 10^{-11}$ (90% CL) for $m_{A^0} < 800$ keV.
[43] The TSUCHIAKI 90 limit is based on inclusive photon spectrum and is independent of A^0 decay modes.
[44] ORITO 89 limit translates to $g^2_{A^0 ee}/4\pi < 6.2 \times 10^{-10}$. Somewhat more sensitive limits are obtained for larger m_{A^0}: $B < 7.6 \times 10^{-6}$ at 100 keV.
[45] AMALDI 85 set limits B($A^0\gamma$) / B($\gamma\gamma\gamma$) < (1–5) $\times 10^{-6}$ for m_{A^0} = 900–100 keV which are about 1/10 of the CARBONI 83 limits.
[46] CARBONI 83 looked for orthopositronium $\to A^0\gamma$. Set limit for A^0 electron coupling squared, $g(eeA^0)^2/(4\pi) < 6. \times 10^{-10}$–$7. \times 10^{-9}$ for m_{A^0} from 150–900 keV (CL = 99.7%). This is about 1/10 of the bound from g–2 experiments.

A^0 (Axion) Search in Photoproduction

VALUE	DOCUMENT ID		COMMENT
• • • We do not use the following data for averages, fits, limits, etc. • • •			
	[47] BASSOMPIE...	95	$m_{A^0} = 1.8 \pm 0.2$ MeV

[47] BASSOMPIERRE 95 is an extension of BASSOMPIERRE 93. They looked for a peak in the invariant mass of e^+e^- pairs in the region $m_{e^+e^-} = 1.8 \pm 0.2$ MeV. They obtained bounds on the production rate A^0 for $\tau(A^0) = 10^{-18}$–10^{-9} sec. They also found an excess of events in the range $m_{e^+e^-}$ = 2.1–3.5 MeV.

A^0 (Axion) Production in Hadron Collisions

Limits are for $\sigma(A^0)$ / $\sigma(\pi^0)$.

VALUE	CL%	EVTS	DOCUMENT ID		TECN	COMMENT
• • • We do not use the following data for averages, fits, limits, etc. • • •						
			[48] JAIN	07	CNTR	$A^0 \to e^+e^-$
			[49] AHMAD	97	SPEC	e^+ production
			[50] LEINBERGER	97	SPEC	$A^0 \to e^+e^-$
			[51] GANZ	96	SPEC	$A^0 \to e^+e^-$
			[52] KAMEL	96	EMUL	^{32}S emulsion, $A^0 \to e^+e^-$
			[53] BLUEMLEIN	92	BDMP	$A^0 N_Z \to \ell^+\ell^- N_Z$
			[54] MEIJERDREES	92	SPEC	$\pi^- p \to nA^0$, $A^0 \to e^+e^-$
			[55] BLUEMLEIN	91	BDMP	$A^0 \to e^+e^-$, 2γ
			[56] FAISSNER	89	OSPK	Beam dump, $A^0 \to e^+e^-$
			[57] DEBOER	88	RVUE	$A^0 \to e^+e^-$
			[58] EL-NADI	88	EMUL	$A^0 \to e^+e^-$
			[59] FAISSNER	88	OSPK	Beam dump, $A^0 \to 2\gamma$
			[60] BADIER	86	BDMP	$A^0 \to e^+e^-$
$<2. \times 10^{-11}$	90	0	[61] BERGSMA	85	CHRM	CERN beam dump
$<1. \times 10^{-13}$	90	0	[61] BERGSMA	85	CHRM	CERN beam dump
		24	[62] FAISSNER	83	OSPK	Beam dump, $A^0 \to 2\gamma$
			[63] FAISSNER	83B	RVUE	LAMPF beam dump
			[64] FRANK	83B	RVUE	LAMPF beam dump
			[65] HOFFMAN	83	CNTR	$\pi p \to nA^0$ ($A^0 \to e^+e^-$)
			[66] FETSCHER	82	RVUE	See FAISSNER 81B
		12	[67] FAISSNER	81	OSPK	CERN PS ν wideband
		15	[68] FAISSNER	81B	OSPK	Beam dump, $A^0 \to 2\gamma$
		8	[69] KIM	81	OSPK	26 GeV $pN \to A^0 X$
		0	[70] FAISSNER	80	OSPK	Beam dump, $A^0 \to e^+e^-$
$<1. \times 10^{-8}$	90		[71] JACQUES	80	HLBC	28 GeV protons
$<1. \times 10^{-14}$	90		[71] JACQUES	80	HLBC	Beam dump
			[72] SOUKAS	80	CALO	28 GeV p beam dump
			[73] BECHIS	79	CNTR	
$<1. \times 10^{-8}$	90		[74] COTEUS	79	OSPK	Beam dump
$<1. \times 10^{-3}$	95		[75] DISHAW	79	CALO	400 GeV pp
$<1. \times 10^{-8}$	90		ALIBRAN	78	HYBR	Beam dump
$<6. \times 10^{-9}$	95		ASRATYAN	78B	CALO	Beam dump
$<1.5 \times 10^{-8}$	90		[76] BELLOTTI	78	HLBC	Beam dump
$<5.4 \times 10^{-14}$	90		[76] BELLOTTI	78	HLBC	m_{A^0}=1.5 MeV
$<4.1 \times 10^{-9}$	90		[76] BELLOTTI	78	HLBC	m_{A^0}=1 MeV
$<1. \times 10^{-8}$	90		[77] BOSETTI	78B	HYBR	Beam dump
			[78] DONNELLY	78		
$<0.5 \times 10^{-8}$	90		HANSL	78D	WIRE	Beam dump
			[79] MICELMAC...	78		
			[80] VYSOTSKII	78		

[48] JAIN 07 claims evidence for $A^0 \to e^+e^-$ produced in ^{207}Pb collision on nuclear emulsion (Ag/Br) for $m(A^0) = 7 \pm 1$ or 19 ± 1 MeV and $\tau(A^0) \leq 10^{-13}$ s.
[49] AHMAD 97 reports a result of APEX Collaboration which studied positron production in ^{238}U+^{232}Ta and ^{238}U+^{181}Ta collisions, without requiring a coincident electron. No narrow lines were found for 250 < E_{e^+} < 750 keV.
[50] LEINBERGER 97 (ORANGE Collaboration) at GSI looked for a narrow sum-energy e^+e^--line at $\sim$ 635 keV in ^{238}U+^{181}Ta collision. Limits on the production probability for a narrow sum-energy e^+e^- line are set. See their Table 2.
[51] GANZ 96 (EPos II Collaboration) has placed upper bounds on the production cross section of e^+e^- pairs from ^{238}U+^{181}Ta and ^{238}U+^{232}Th collisions at GSI. See Table 2 for limits both for back-to-back and isotropic configurations of e^+e^- pairs. These limits rule out the existence of peaks in the e^+e^- sum-energy distribution, reported by an earlier version of this experiment.
[52] KAMEL 96 looked for e^+e^- pairs from the collision of ^{32}S (200 GeV/nucleon) and emulsion. No evidence of mass peaks is found in the region of sensitivity m_{ee} >2 MeV.
[53] BLUEMLEIN 92 is a proton beam dump experiment at Serpukhov with a secondary target to induce Bethe-Heitler production of e^+e^- or $\mu^+\mu^-$ from the produce A^0. See Fig. 5 for the excluded region in m_{A^0}-x plane. For the standard axion, 0.3 <x<25 is excluded at 95% CL. If combined with BLUEMLEIN 91, 0.008 <x<32 is excluded.
[54] MEIJERDREES 92 give $\Gamma(\pi^- p \to nA^0)\cdot B(A^0 \to e^+e^-)/\Gamma(\pi^- p \to \text{all}) < 10^{-5}$ (90% CL) for m_{A^0} = 100 MeV, $\tau_{A^0} = 10^{-11}$–10^{-23} sec. Limits ranging from 2.5×10^{-3} to 10^{-7} are given for m_{A^0} = 25–136 MeV.
[55] BLUEMLEIN 91 is a proton beam dump experiment at Serpukhov. No candidate event for $A^0 \to e^+e^-$, 2γ are found. Fig. 6 gives the excluded region in m_{A^0}-x plane ($x = \tan\beta = v_2/v_1$). Standard axion is excluded for 0.2 < m_{A^0} < 3.2 MeV for most $x > 1$, 0.2–11 MeV for most $x < 1$.
[56] FAISSNER 89 searched for $A^0 \to e^+e^-$ in a proton beam dump experiment at SIN. No excess of events was observed over the background. A standard axion with mass $2m_e$–20 MeV is excluded. Lower limit on f_{A^0} of $\simeq 10^4$ GeV is given for $m_{A^0} = 2m_e$–20 MeV.
[57] DEBOER 88 reanalyze EL-NADI 88 data and claim evidence for three distinct states with mass $\sim$ 1.1, $\sim$ 2.1, and $\sim$ 9 MeV, lifetimes 10^{-16}–10^{-15} s decaying to e^+e^- and note the similarity of the data with those of a cosmic-ray experiment by Bristol group (B.M. Anand, Proc. of the Royal Society of London, Section A **A22** 183 (1953)). For a criticism see PERKINS 89, who suggests that the events are compatible with π^0 Dalitz decay. DEBOER 89B is a reply which contests the criticism.
[58] EL-NADI 88 claim the existence of a neutral particle decaying into e^+e^- with mass 1.60 $\pm$ 0.59 MeV, lifetime (0.15 $\pm$ 0.01) $\times 10^{-14}$ s, which is produced in heavy ion interactions with emulsion nuclei at $\sim$ 4 GeV/c/nucleon.
[59] FAISSNER 88 is a proton beam dump experiment at SIN. They found no candidate event for $A^0 \to \gamma\gamma$. A standard axion decaying to 2γ is excluded except for a region $x \simeq 1$. Lower limit on f_{A^0} of 10^2–10^3 GeV is given for m_{A^0} = 0.1–1 MeV.
[60] BADIER 86 did not find long-lived A^0 in 300 GeV π^- Beam Dump Experiment that decays into e^+e^- in the mass range m_{A^0} = (20–200) MeV, which excludes the A^0 decay constant $f(A^0)$ in the interval (60–600) GeV. See their figure 6 for excluded region on $f(A^0)$-m_{A^0} plane.
[61] BERGSMA 85 look for $A^0 \to 2\gamma$, e^+e^-, $\mu^+\mu^-$. First limit above is for m_{A^0} = 1 MeV; second is for 200 MeV. See their figure 4 for excluded region on f_{A^0}–m_{A^0} plane, where f_{A^0} is A^0 decay constant. For Peccei-Quinn PECCEI 77 A^0, m_{A^0} <180 keV and τ >0.037 s. (CL = 90%). For the axion of FAISSNER 81B at 250 keV, BERGSMA 85 expect 15 events but observe zero.

[62] FAISSNER 83 observed 19 1-γ and 12 2-γ events where a background of 4.8 and 2.3 respectively is expected. A small-angle peak is observed even if iron wall is set in front of the decay region.

[63] FAISSNER 83B extrapolate SIN γ signal to LAMPF ν experimental condition. Resulting 370 γ's are not at variance with LAMPF upper limit of 450 γ's. Derived from LAMPF limit that $[d\sigma(A^0)/d\omega$ at $90°]m_{A^0}/\tau_{A^0} < 14 \times 10^{-35}$ cm^2 sr^{-1} MeV ms^{-1}. See comment on FRANK 83B.

[64] FRANK 83B stress the importance of LAMPF data bins with negative net signal. By statistical analysis say that LAMPF and SIN-A0 are at variance when extrapolation by phase-space model is done. They find LAMPF upper limit is 248 not 450 γ's. See comment on FAISSNER 83B.

[65] HOFFMAN 83 set CL = 90% limit $d\sigma/dt$ B$(e^+e^-) < 3.5 \times 10^{-32}$ cm^2/GeV^2 for 140 $< m_{A^0} <$160 MeV. Limit assumes $\tau(A^0) < 10^{-9}$ s.

[66] FETSCHER 82 reanalyzes SIN beam-dump data of FAISSNER 81. Claims no evidence for axion since 2-γ peak rate remarkably decreases if iron wall is set in front of the decay region.

[67] FAISSNER 81 see excess μe events. Suggest axion interactions.

[68] FAISSNER 81B is SIN 590 MeV proton beam dump. Observed 14.5 ± 5.0 events of 2γ decay of long-lived neutral penetrating particle with $m_{2\gamma} \lesssim 1$ MeV. Axion interpretation with η-A^0 mixing gives $m_{A^0} = 250 \pm 25$ keV, $\tau_{(2\gamma)} = (7.3 \pm 3.7) \times 10^{-3}$ s from above rate. See critical remarks below in comments of FETSCHER 82, FAISSNER 83, FAISSNER 83B, FRANK 83B, and BERGSMA 85. Also see in the next subsection ALEKSEEV 82B, CAVAIGNAC 83, and ANANEV 85.

[69] KIM 81 analyzed 8 candidates for $A^0 \rightarrow 2\gamma$ obtained by Aachen-Padova experiment at CERN with 26 GeV protons on Be. Estimated axion mass is about 300 keV and lifetime is (0.86∼ 5.6) $\times 10^{-3}$ s depending on models. Faissner (private communication), says axion production underestimated and mass overestimated. Correct value around 200 keV.

[70] FAISSNER 80 is SIN beam dump experiment with 590 MeV protons looking for $A^0 \rightarrow e^+e^-$ decay. Assuming $A^0/\pi^0 = 5.5 \times 10^{-7}$, obtained decay rate limit 20/(A^0 mass) MeV/s (CL = 90%), which is about 10^{-7} below theory and interpreted as upper limit to $m_{A^0} < 2m_{e^-}$.

[71] JACQUES 80 is a BNL beam dump experiment. First limit above comes from nonobservation of excess neutral-current-type events $[\sigma(\text{production})\sigma(\text{interaction}) < 7. \times 10^{-68}$ cm^4, CL = 90%$]$. Second limit is from nonobservation of axion decays into 2γ's or e^+e^-, and for axion mass a few MeV.

[72] SOUKAS 80 at BNL observed no excess of neutral-current-type events in beam dump.

[73] BECHIS 79 looked for the axion production in low energy electron Bremsstrahlung and the subsequent decay into either 2γ or e^+e^-. No signal found. CL = 90% limits for model parameter(s) are given.

[74] COTEUS 79 is a beam dump experiment at BNL.

[75] DISHAW 79 is a calorimetric experiment and looks for low energy tail of energy distributions due to energy lost to weakly interacting particles.

[76] BELLOTTI 78 first value comes from search for $A^0 \rightarrow e^+e^-$. Second value comes from search for $A^0 \rightarrow 2\gamma$, assuming mass $< 2m_{e^-}$. For any mass satisfying this, limit is above value$\times$(mass^{-4}). Third value uses data of PL 60B 401 and quotes $\sigma(\text{production})\sigma(\text{interaction}) < 10^{-67}$ cm^4.

[77] BOSETTI 78B quotes $\sigma(\text{production})\sigma(\text{interaction}) < 2. \times 10^{-67}$ cm^4.

[78] DONNELLY 78 examines data from reactor neutrino experiments of REINES 76 and GURR 74 as well as SLAC beam dump experiment. Evidence is negative.

[79] MICELMACHER 78 finds no evidence of axion existence in reactor experiments of REINES 76 and GURR 74. (See reference under DONNELLY 78 below).

[80] VYSOTSKII 78 derived lower limit for the axion mass 25 keV from luminosity of the sun and 200 keV from red supergiants.

A^0 (Axion) Searches in Reactor Experiments

VALUE	DOCUMENT ID		TECN	COMMENT
• • • We do not use the following data for averages, fits, limits, etc. • • •				
	[81] CHANG	07		Primakoff or Compton
	[82] ALTMANN	95	CNTR	Reactor; $A^0 \rightarrow e^+e^-$
	[83] KETOV	86	SPEC	Reactor, $A^0 \rightarrow \gamma\gamma$
	[84] KOCH	86	SPEC	Reactor; $A^0 \rightarrow \gamma\gamma$
	[85] DATAR	82	CNTR	Light water reactor
	[86] VUILLEUMIER	81	CNTR	Reactor, $A^0 \rightarrow 2\gamma$

[81] CHANG 07 looked for monochromatic photons from Primakoff or Compton conversion of axions from the Kuo-Sheng reactor due to axion coupling to photon or electron, respectively. The search places model-independent limits on the products $G_{A\gamma\gamma}G_{ANN}$ and $G_{Aee}G_{ANN}$ for $m(A^0)$ less than the MeV range.

[82] ALTMANN 95 looked for A^0 decaying into e^+e^- from the Bugey5 nuclear reactor. They obtain an upper limit on the A^0 production rate of $\omega(A^0)/\omega(\gamma)$ $\times$B$(A^0 \rightarrow e^+e^-) < 10^{-16}$ for $m_{A^0} = 1.5$ MeV at 90% CL. The limit is weaker for heavier A^0. In the case of a standard axion, this limit excludes a mass in the range $2m_e < m_{A^0} < 4.8$ MeV at 90% CL. See Fig. 5 of their paper for exclusion limits of axion-like resonances Z^0 in the (m_{X^0}, f_{X^0}) plane.

[83] KETOV 86 searched for A^0 at the Rovno nuclear power plant. They found an upper limit on the A^0 production probability of 0.8 $[100 \text{ keV}/m_{A^0}]^6 \times 10^{-6}$ per fission. In the standard axion model, this corresponds to $m_{A^0} >$150 keV. Not valid for $m_{A^0} \gtrsim$ 1 MeV.

[84] KOCH 86 searched for $A^0 \rightarrow \gamma\gamma$ at nuclear power reactor Biblis A. They found an upper limit on the A^0 production rate of $\omega(A^0)/\omega(\gamma(M1)) < 1.5 \times 10^{-10}$ (CL=95%). Standard axion with $m_{A^0} = 250$ keV gives 10^{-5} for the ratio. Not valid for $m_{A^0} >$1022 keV.

[85] DATAR 82 looked for $A^0 \rightarrow 2\gamma$ in neutron capture ($np \rightarrow dA^0$) at Tarapur 500 MW reactor. Sensitive to sum of $I = 0$ and $I = 1$ amplitudes. With ZEHNDER 81 $[(I = 0) - (I = 1)]$ result, assert nonexistence of standard A^0.

[86] VUILLEUMIER 81 is at Grenoble reactor. Set limit $m_{A^0} <$280 keV.

A^0 (Axion) and Other Light Boson (X^0) Searches in Nuclear Transitions

Limits are for branching ratio.

VALUE	CL%	DOCUMENT ID		TECN	COMMENT
• • • We do not use the following data for averages, fits, limits, etc. • • •					
$< 8.5 \times 10^{-6}$	90	[87] DERBIN	02	CNTR	^{125m}Te decay
		[88] DEBOER	97C	RVUE	M1 transitions
$< 5.5 \times 10^{-10}$	95	[89] TSUNODA	95	CNTR	^{252}Cf fission, $A^0 \rightarrow ee$
$< 1.2 \times 10^{-6}$	95	[90] MINOWA	93	CNTR	^{139}La$^* \rightarrow {}^{139}$LaA^0
$< 2 \times 10^{-4}$	90	[91] HICKS	92	CNTR	^{35}S decay, $A^0 \rightarrow \gamma\gamma$
$< 1.5 \times 10^{-9}$	95	[92] ASANUMA	90	CNTR	^{241}Am decay
$<(0.4\text{–}10) \times 10^{-3}$	95	[93] DEBOER	90	CNTR	^{8}Be$^* \rightarrow {}^8$BeA^0, $A^0 \rightarrow e^+e^-$
$<(0.2\text{–}1) \times 10^{-3}$	90	[94] BINI	89	CNTR	^{16}O$^* \rightarrow {}^{16}$OX^0, $X^0 \rightarrow e^+e^-$
		[95] AVIGNONE	88	CNTR	Cu$^* \rightarrow$ CuA^0 ($A^0 \rightarrow 2\gamma$, $A^0 e \rightarrow \gamma e$, $A^0 Z \rightarrow \gamma Z$)
$< 1.5 \times 10^{-4}$	90	[96] DATAR	88	CNTR	^{12}C$^* \rightarrow {}^{12}$CA^0, $A^0 \rightarrow e^+e^-$
$< 5 \times 10^{-3}$	90	[97] DEBOER	88C	CNTR	^{16}O$^* \rightarrow {}^{16}$OX^0, $X^0 \rightarrow e^+e^-$
$< 3.4 \times 10^{-5}$	95	[98] DOEHNER	88	SPEC	^{2}H*, $A^0 \rightarrow e^+e^-$
$< 4 \times 10^{-4}$	95	[99] SAVAGE	88	CNTR	Nuclear decay (isovector)
$< 3 \times 10^{-3}$	95	[99] SAVAGE	88	CNTR	Nuclear decay (isoscalar)
$<10.6 \times 10^{-2}$	90	[100] HALLIN	86	SPEC	^{6}Li isovector decay
<10.8	90	[100] HALLIN	86	SPEC	^{10}B isoscalar decays
< 2.2	90	[100] HALLIN	86	SPEC	^{14}N isoscalar decays
$< 4 \times 10^{-4}$	90	[101] SAVAGE	86B	CNTR	^{14}N*
		[102] ANANEV	85	CNTR	Li*, deut* $A^0 \rightarrow 2\gamma$
		[103] CAVAIGNAC	83	CNTR	^{97}Nb*, deut* transition $A^0 \rightarrow 2\gamma$
		[104] ALEKSEEV	82B	CNTR	Li*, deut* transition $A^0 \rightarrow 2\gamma$
		[105] LEHMANN	82	CNTR	Cu$^* \rightarrow$ CuA^0 ($A^0 \rightarrow 2\gamma$)
		[106] ZEHNDER	82	CNTR	Li*, Nb* decay, n-capt.
		[107] ZEHNDER	81	CNTR	Ba$^* \rightarrow$ BaA^0 ($A^0 \rightarrow 2\gamma$)
		[108] CALAPRICE	79		Carbon

[87] DERBIN 02 looked for the axion emission in an M1 transition in ^{125m}Te decay. They looked for a possible presence of a shifted energy spectrum in gamma rays due to the undetected axion.

[88] DEBOER 97C reanalyzed the existent data on Nuclear M1 transitions and find that a 9 MeV boson decaying into e^+e^- would explain the excess of events with large opening angles. See also DEBOER 01 for follow-up experiments.

[89] TSUNODA 95 looked for axion emission when ^{252}Cf undergoes a spontaneous fission, with the axion decaying into e^+e^-. The bound is for m_{A^0}=40 MeV. It improves to 2.5×10^{-5} for m_{A^0}=200 MeV.

[90] MINOWA 93 studied chain process, ^{139}Ce $\rightarrow$ ^{139}La* by electron capture and M1 transition of ^{139}La* to the ground state. It does not assume decay modes of A^0. The bound applies for $m_{A^0} < 166$ keV.

[91] HICKS 92 bound is applicable for $\tau_{X^0} < 4 \times 10^{-11}$ sec.

[92] The ASANUMA 90 limit is for the branching fraction of X^0 emission per ^{241}Amα decay and valid for $\tau_{X^0} < 3 \times 10^{-11}$ s.

[93] The DEBOER 90 limit is for the branching ratio ^{8}Be* (18.15 MeV, 1^+) $\rightarrow$ ^{8}BeA^0, $A^0 \rightarrow e^+e^-$ for the mass range $m_{A^0} = 4$–15 MeV.

[94] The BINI 89 limit is for the branching fraction of ^{16}O*(6.05 MeV, 0^+) $\rightarrow$ ^{16}OX^0, $X^0 \rightarrow e^+e^-$ for $m_X = 1.5$–3.1 MeV. $\tau_{X^0} \lesssim 10^{-11}$ s is assumed. The spin-parity of X is restricted to 0^+ or 1^-.

[95] AVIGNONE 88 looked for the 1115 keV transition C$^* \rightarrow$ CuA^0, either from $A^0 \rightarrow 2\gamma$ in-flight decay or from the secondary A^0 interactions by Compton and by Primakoff processes. Limits for axion parameters are obtained for $m_{A^0} < 1.1$ MeV.

[96] DATAR 88 rule out light pseudoscalar particle emission through its decay $A^0 \rightarrow e^+e^-$ in the mass range 1.02–2.5 MeV and lifetime range 10^{-13}–10^{-8} s. The above limit is for $\tau = 5 \times 10^{-13}$ s and $m = 1.7$ MeV; see the paper for the τ-m dependence of the limit.

[97] The limit is for the branching fraction of ^{16}O*(6.05 MeV, 0^+) $\rightarrow$ ^{16}OX^0, $X^0 \rightarrow e^+e^-$ against internal pair conversion for $m_{X^0} = 1.7$ MeV and $\tau_{X^0} < 10^{-11}$ s. Similar limits are obtained for $m_{X^0} = 1.3$–3.2 MeV. The spin parity of X^0 must be either 0^+ or 1^-. The limit at 1.7 MeV is translated into a limit for the X^0-nucleon coupling constant: $g^2_{X^0NN}/4\pi < 2.3 \times 10^{-9}$.

[98] The DOEHNER 88 limit is for $m_{A^0} = 1.7$ MeV, $\tau(A^0) < 10^{-10}$ s. Limits less than 10^{-4} are obtained for $m_{A^0} = 1.2$–2.2 MeV.

[99] SAVAGE 88 looked for A^0 that decays into e^+e^- in the decay of the 9.17 MeV $J^P = 2^+$ state in ^{14}N, 17.64 MeV state $J^P = 1^+$ in ^{8}Be, and the 18.15 MeV state $J^P = 1^+$ in ^{8}Be. This experiment constrains the isovector coupling of A^0 to hadrons, if m_{A^0} = (1.1 $\rightarrow$ 2.2) MeV and the isoscalar coupling of A^0 to hadrons, if m_{A^0} = (1.1 $\rightarrow$ 2.6) MeV. Both limits are valid only if $\tau(A^0) \lesssim 1 \times 10^{-11}$ s.

[100] Limits are for $\Gamma(A^0(1.8 \text{ MeV}))/\Gamma(\pi M1)$; i.e., for 1.8 MeV axion emission normalized to the rate for internal emission of e^+e^- pairs. Valid for $\tau_{A^0} < 2 \times 10^{-11}$s. ^{6}Li isovector decay data strongly disfavor PECCEI 86 model I, whereas the ^{10}B and ^{14}N isoscalar decay data strongly reject PECCEI 86 model II and III.

[101] SAVAGE 86B looked for A^0 that decays into e^+e^- in the decay of the 9.17 MeV $J^P = 2^+$ state in ^{14}N. Limit on the branching fraction is valid if $\tau_{A^0} \lesssim 1. \times 10^{-11}$s for $m_{A^0} = (1.1–1.7)$ MeV. This experiment constrains the iso-vector coupling of A^0 to hadrons.
[102] ANANEV 85 with IBR-2 pulsed reactor exclude standard A^0 at CL = 95% masses below 470 keV (Li* decay) and below $2m_e$ for deuteron* decay.
[103] CAVAIGNAC 83 at Bugey reactor exclude axion at any $m_{^{97}\text{Nb}^*\text{decay}}$ and axion with m_{A^0} between 275 and 288 keV (deuteron* decay).
[104] ALEKSEEV 82 with IBR-2 pulsed reactor exclude standard A^0 at CL = 95% mass-ranges m_{A^0} <400 keV (Li* decay) and 330 keV $< m_{A^0}$ <2.2 MeV. (deuteron* decay).
[105] LEHMANN 82 obtained $A^0 \rightarrow 2\gamma$ rate $< 6.2 \times 10^{-5}$/s (CL = 95%) excluding m_{A^0} between 100 and 1000 keV.
[106] ZEHNDER 82 used Gosgen 2.8GW light-water reactor to check A^0 production. No 2γ peak in Li*, Nb* decay (both single p transition) nor in n capture (combined with previous Ba* negative result) rules out standard A^0. Set limit m_{A^0} <60 keV for any A^0.
[107] ZEHNDER 81 looked for Ba* $\rightarrow$ A^0Ba transition with $A^0 \rightarrow 2\gamma$. Obtained 2γ coincidence rate $< 2.2 \times 10^{-5}$/s (CL = 95%) excluding m_{A^0} >160 keV (or 200 keV depending on Higgs mixing). However, see BARROSO 81.
[108] CALAPRICE 79 saw no axion emission from excited states of carbon. Sensitive to axion mass between 1 and 15 MeV.

A^0 (Axion) Limits from Its Electron Coupling

Limits are for $\tau(A^0 \rightarrow e^+e^-)$.

VALUE (s)	CL%	DOCUMENT ID		TECN	COMMENT
• • • We do not use the following data for averages, fits, limits, etc. • • •					
none 4×10^{-16}–4.5×10^{-12}	90	[109] BROSS	91	BDMP	$eN \rightarrow eA^0N$ ($A^0 \rightarrow ee$)
		[110] GUO	90	BDMP	$eN \rightarrow eA^0N$ ($A^0 \rightarrow ee$)
		[111] BJORKEN	88	CALO	$A \rightarrow e^+e^-$ or 2γ
		[112] BLINOV	88	MD1	$ee \rightarrow eeA^0$ ($A^0 \rightarrow ee$)
none 1×10^{-14}–1×10^{-10}	90	[113] RIORDAN	87	BDMP	$eN \rightarrow eA^0N$ ($A^0 \rightarrow ee$)
none 1×10^{-14}–1×10^{-11}	90	[114] BROWN	86	BDMP	$eN \rightarrow eA^0N$ ($A^0 \rightarrow ee$)
none 6×10^{-14}–9×10^{-11}	95	[115] DAVIER	86	BDMP	$eN \rightarrow eA^0N$ ($A^0 \rightarrow ee$)
none 3×10^{-13}–1×10^{-7}	90	[116] KONAKA	86	BDMP	$eN \rightarrow eA^0N$ ($A^0 \rightarrow ee$)

[109] The listed BROSS 91 limit is for $m_{A^0} = 1.14$ MeV. B($A^0 \rightarrow e^+e^-$) = 1 assumed. Excluded domain in the τ_{A^0}–m_{A^0} plane extends up to $m_{A^0} \approx 7$ MeV (see Fig. 5). Combining with electron $g-2$ constraint, axions coupling only to e^+e^- ruled out for $m_{A^0} < 4.8$ MeV (90% CL).
[110] GUO 90 use the same apparatus as BROWN 86 and improve the previous limit in the shorter lifetime region. Combined with $g-2$ constraint, axions coupling only to e^+e^- are ruled out for $m_{A^0} < 2.7$ MeV (90% CL).
[111] BJORKEN 88 reports limits on axion parameters (f_A, m_A, τ_A) for m_{A^0} < 200 MeV from electron beam-dump experiment with production via Primakoff photoproduction, bremsstrahlung from electrons, and resonant annihilation of positrons on atomic electrons.
[112] BLINOV 88 assume zero spin, m = 1.8 MeV and lifetime < 5×10^{-12} s and find $\Gamma(A^0 \rightarrow \gamma\gamma)$B($A^0 \rightarrow e^+e^-$) < 2 eV (CL=90%).
[113] Assumes $A^0\gamma\gamma$ coupling is small and hence Primakoff production is small. Their figure 2 shows limits on axions for m_{A^0} < 15 MeV.
[114] Uses electrons in hadronic showers from an incident 800 GeV proton beam. Limits for m_{A^0} < 15 MeV are shown in their figure 3.
[115] m_{A^0} = 1.8 MeV assumed. The excluded domain in the $\tau_{A^0}-m_{A^0}$ plane extends up to $m_{A^0} \approx 14$ MeV, see their figure 4.
[116] The limits are obtained from their figure 3. Also given is the limit on the $A^0\gamma\gamma$–$A^0e^+e^-$ coupling plane by assuming Primakoff production.

Search for A^0 (Axion) Resonance in Bhabha Scattering

The limit is for $\Gamma(A^0)[\text{B}(A^0 \rightarrow e^+e^-)]^2$.

VALUE (10^{-3} eV)	CL%	DOCUMENT ID		TECN	COMMENT
• • • We do not use the following data for averages, fits, limits, etc. • • •					
< 1.3	97	[117] HALLIN	92	CNTR	m_{A^0} = 1.75–1.88 MeV
none 0.0016–0.47	90	[118] HENDERSON	92C	CNTR	m_{A^0}= 1.5–1.86 MeV
< 2.0	90	[119] WU	92	CNTR	m_{A^0}= 1.56–1.86 MeV
< 0.013	95	TSERTOS	91	CNTR	m_{A^0} = 1.832 MeV
none 0.19–3.3	95	[120] WIDMANN	91	CNTR	m_{A^0}= 1.78–1.92 MeV
< 5	97	BAUER	90	CNTR	m_{A^0} = 1.832 MeV
none 0.09–1.5	95	[121] JUDGE	90	CNTR	m_{A^0} = 1.832 MeV, elastic
< 1.9	97	[122] TSERTOS	89	CNTR	m_{A^0} = 1.82 MeV
<(10–40)	97	[122] TSERTOS	89	CNTR	m_{A^0} = 1.51–1.65 MeV
<(1–2.5)	97	[122] TSERTOS	89	CNTR	m_{A^0} = 1.80–1.86 MeV
< 31	95	LORENZ	88	CNTR	m_{A^0} = 1.646 MeV
< 94	95	LORENZ	88	CNTR	m_{A^0} = 1.726 MeV
< 23	95	LORENZ	88	CNTR	m_{A^0} = 1.782 MeV
< 19	95	LORENZ	88	CNTR	m_{A^0} = 1.837 MeV
< 3.8	97	[123] TSERTOS	88	CNTR	m_{A^0} = 1.832 MeV
		[124] VANKLINKEN	88	CNTR	
		[125] MAIER	87	CNTR	
<2500	90	MILLS	87	CNTR	m_{A^0} = 1.8 MeV
		[126] VONWIMMER.	87	CNTR	

[117] HALLIN 92 quote limits on lifetime, $8 \times 10^{-14} - 5 \times 10^{-13}$ sec depending on mass, assuming B($A^0 \rightarrow e^+e^-$) = 100%. They say that TSERTOS 91 overstated their sensitivity by a factor of 3.
[118] HENDERSON 92C exclude axion with lifetime $\tau_{A^0}=1.4 \times 10^{-12} - 4.0 \times 10^{-10}$ s, assuming B($A^0 \rightarrow e^+e^-$)=100%. HENDERSON 92C also exclude a vector boson with $\tau=1.4 \times 10^{-12} - 6.0 \times 10^{-10}$ s.
[119] WU 92 quote limits on lifetime > 3.3×10^{-13} s assuming B($A^0 \rightarrow e^+e^-$)=100%. They say that TSERTOS 89 overestimate the limit by a factor of $\pi/2$. WU 92 also quote a bound for vector boson, $\tau > 8.2 \times 10^{-13}$ s.
[120] WIDMANN 91 bound applies exclusively to the case B($A^0 \rightarrow e^+e^-$)=1, since the detection efficiency varies substantially as $\Gamma(A^0)_{\text{total}}$ changes. See their Fig. 6.
[121] JUDGE 90 excludes an elastic pseudoscalar e^+e^- resonance for 4.5×10^{-13} s < $\tau(A^0)$ < 7.5×10^{-12} s (95% CL) at m_{A^0} = 1.832 MeV. Comparable limits can be set for m_{A^0} = 1.776–1.856 MeV.
[122] See also TSERTOS 88B in references.
[123] The upper limit listed in TSERTOS 88 is too large by a factor of 4. See TSERTOS 88B, footnote 3.
[124] VANKLINKEN 88 looked for relatively long-lived resonance ($\tau = 10^{-10}$–10^{-12} s). The sensitivity is not sufficient to exclude such a narrow resonance.
[125] MAIER 87 obtained limits $R\Gamma \lesssim 60$ eV (100 eV) at $m_{A^0} \simeq 1.64$ MeV (1.83 MeV) for energy resolution $\Delta E_{\text{cm}} \simeq 3$ keV, where R is the resonance cross section normalized to that of Bhabha scattering, and $\Gamma = \Gamma^2_{ee}/\Gamma_{\text{total}}$. For a discussion implying that $\Delta E_{\text{cm}} \simeq 10$ keV, see TSERTOS 89.
[126] VONWIMMERSPERG 87 measured Bhabha scattering for E_{cm} = 1.37–1.86 MeV and found a possible peak at 1.73 with $\int \sigma dE_{\text{cm}} = 14.5 \pm 6.8$ keV·b. For a comment and a reply, see VANKLINKEN 88B and VONWIMMERSPERG 88. Also see CONNELL 88.

Search for A^0 (Axion) Resonance in $e^+e^- \rightarrow \gamma\gamma$

The limit is for $\Gamma(A^0 \rightarrow e^+e^-)\cdot\Gamma(A^0 \rightarrow \gamma\gamma)/\Gamma_{\text{total}}$

VALUE (10^{-3} eV)	CL%	DOCUMENT ID		TECN	COMMENT
• • • We do not use the following data for averages, fits, limits, etc. • • •					
< 0.18	95	VO	94	CNTR	m_{A^0}=1.1 MeV
< 1.5	95	VO	94	CNTR	m_{A^0}=1.4 MeV
<12	95	VO	94	CNTR	m_{A^0}=1.7 MeV
< 6.6	95	[127] TRZASKA	91	CNTR	m_{A^0} = 1.8 MeV
< 4.4	95	WIDMANN	91	CNTR	m_{A^0}= 1.78–1.92 MeV
		[128] FOX	89	CNTR	
< 0.11	95	[129] MINOWA	89	CNTR	m_{A^0} = 1.062 MeV
<33	97	CONNELL	88	CNTR	m_{A^0} = 1.580 MeV
<42	97	CONNELL	88	CNTR	m_{A^0} = 1.642 MeV
<73	97	CONNELL	88	CNTR	m_{A^0} = 1.782 MeV
<79	97	CONNELL	88	CNTR	m_{A^0} = 1.832 MeV

[127] TRZASKA 91 also give limits in the range (6.6–30) $\times 10^{-3}$ eV (95%CL) for m_{A^0} = 1.6–2.0 MeV.
[128] FOX 89 measured positron annihilation with an electron in the source material into two photons and found no signal at 1.062 MeV (< 9×10^{-5} of two-photon annihilation at rest).
[129] Similar limits are obtained for m_{A^0} = 1.045–1.085 MeV.

Search for X^0 (Light Boson) Resonance in $e^+e^- \rightarrow \gamma\gamma\gamma$

The limit is for $\Gamma(X^0 \rightarrow e^+e^-)\cdot\Gamma(X^0 \rightarrow \gamma\gamma\gamma)/\Gamma_{\text{total}}$. C invariance forbids spin-0 X^0 coupling to both e^+e^- and $\gamma\gamma\gamma$.

VALUE (10^{-3} eV)	CL%	DOCUMENT ID		TECN	COMMENT
• • • We do not use the following data for averages, fits, limits, etc. • • •					
< 0.2	95	[130] VO	94	CNTR	m_{X^0}=1.1–1.9 MeV
< 1.0	95	[131] VO	94	CNTR	m_{X^0}=1.1 MeV
< 2.5	95	[131] VO	94	CNTR	m_{X^0}=1.4 MeV
<120	95	[131] VO	94	CNTR	m_{X^0}=1.7 MeV
< 3.8	95	[132] SKALSEY	92	CNTR	m_{X^0}= 1.5 MeV

[130] VO 94 looked for $X^0 \rightarrow \gamma\gamma\gamma$ decaying at rest. The precise limits depend on m_{X^0}. See Fig. 2(b) in paper.
[131] VO 94 looked for $X^0 \rightarrow \gamma\gamma\gamma$ decaying in flight.
[132] SKALSEY 92 also give limits 4.3 for m_{X^0} = 1.54 and 7.5 for 1.64 MeV. The spin of X^0 is assumed to be one.

Light Boson (X^0) Search in Nonresonant e^+e^- Annihilation at Rest

Limits are for the ratio of $n\gamma + X^0$ production relative to $\gamma\gamma$.

VALUE (units 10^{-6})	CL%	DOCUMENT ID	TECN	COMMENT
• • • We do not use the following data for averages, fits, limits, etc. • • •				

VALUE	CL%	DOCUMENT ID		TECN	COMMENT
< 4.2	90	[133] MITSUI	96	CNTR	γX^0
< 4	68	[134] SKALSEY	95	CNTR	γX^0
<40	68	[135] SKALSEY	95	RVUE	γX^0
< 0.18	90	[136] ADACHI	94	CNTR	$\gamma\gamma X^0$, $X^0 \to \gamma\gamma$
< 0.26	90	[137] ADACHI	94	CNTR	$\gamma\gamma X^0$, $X^0 \to \gamma\gamma$
< 0.33	90	[138] ADACHI	94	CNTR	γX^0, $X^0 \to \gamma\gamma\gamma$

[133] MITSUI 96 looked for a monochromatic γ. The bound applies for a vector X^0 with C=-1 and m_{X^0} <200 keV. They derive an upper bound on $ee X^0$ coupling and hence on the branching ratio B(o-Ps $\to \gamma\gamma X^0$)$< 6.2\times10^{-6}$. The bounds weaken for heavier X^0.

[134] SKALSEY 95 looked for a monochromatic γ without an accompanying γ in e^+e^- annihilation. The bound applies for scalar and vector X^0 with $C = -1$ and m_{X^0} = 100–1000 keV.

[135] SKALSEY 95 reinterpreted the bound on γA^0 decay of o-Ps by ASAI 91 where 3% of delayed annihilations are not from $^3S_1$ states. The bound applies for scalar and vector X^0 with $C = -1$ and m_{X^0} = 0–800 keV.

[136] ADACHI 94 looked for a peak in the $\gamma\gamma$ invariant mass distribution in $\gamma\gamma\gamma\gamma$ production from e^+e^- annihilation. The bound applies for m_{X^0} = 70–800 keV.

[137] ADACHI 94 looked for a peak in the missing-mass mass distribution in $\gamma\gamma$ channel, using $\gamma\gamma\gamma\gamma$ production from e^+e^- annihilation. The bound applies for m_{X^0} <800 keV.

[138] ADACHI 94 looked for a peak in the missing mass distribution in $\gamma\gamma\gamma$ channel, using $\gamma\gamma\gamma\gamma$ production from e^+e^- annihilation. The bound applies for m_{X^0} = 200–900 keV.

Searches for Goldstone Bosons (X^0)

(Including Horizontal Bosons and Majorons.) Limits are for branching ratios.

VALUE	CL%	DOCUMENT ID		TECN	COMMENT
• • • We do not use the following data for averages, fits, limits, etc. • • •					
		[139] LESSA	07	RVUE	Meson, ℓ decays to Majoron
		[140] DIAZ	98	THEO	$H^0 \to X^0X^0$, $A^0 \to X^0X^0X^0$, Majoron
		[141] BOBRAKOV	91		Electron quasi-magnetic interaction
$<3.3\times10^{-2}$	95	[142] ALBRECHT	90E	ARG	$\tau \to \mu X^0$. Familon
$<1.8\times10^{-2}$	95	[142] ALBRECHT	90E	ARG	$\tau \to e X^0$. Familon
$<6.4\times10^{-9}$	90	[143] ATIYA	90	B787	$K^+ \to \pi^+ X^0$. Familon
$<1.1\times10^{-9}$	90	[144] BOLTON	88	CBOX	$\mu^+ \to e^+\gamma X^0$. Familon
		[145] CHANDA	88	ASTR	Sun, Majoron
		[146] CHOI	88	ASTR	Majoron, SN 1987A
$<5\times10^{-6}$	90	[147] PICCIOTTO	88	CNTR	$\pi \to e\nu X^0$, Majoron
$<1.3\times10^{-9}$	90	[148] GOLDMAN	87	CNTR	$\mu \to e\gamma X^0$. Familon
$<3\times10^{-4}$	90	[149] BRYMAN	86B	RVUE	$\mu \to e X^0$. Familon
$<1\times10^{-10}$	90	[150] EICHLER	86	SPEC	$\mu^+ \to e^+ X^0$. Familon
$<2.6\times10^{-6}$	90	[151] JODIDIO	86	SPEC	$\mu^+ \to e^+ X^0$. Familon
		[152] BALTRUSAIT...	85	MRK3	$\tau \to \ell X^0$. Familon
		[153] DICUS	83	COSM	ν(hvy) $\to \nu$(light) X^0

[139] LESSA 07 consider decays of the form Meson $\to \ell\nu$Majoron and $\ell \to \ell'\nu\nu$Majoron and use existing data to derive limits on the neutrino-Majoron Yukawa couplings $g_{\alpha\beta}$ (α,β=e,μ,τ). Their best limits are $|g_{e\alpha}|^2 < 5.5\times10^{-6}$, $|g_{\mu\alpha}|^2 < 4.5\times10^{-5}$, $|g_{\tau\alpha}|^2 < 5.5\times10^{-2}$ at CL = 90%.

[140] DIAZ 98 studied models of spontaneously broken lepton number with both singlet and triplet Higgses. They obtain limits on the parameter space from invisible decay $Z \to H^0A^0 \to X^0X^0X^0X^0X^0$ and $e^+e^- \to ZH^0$ with $H^0 \to X^0X^0$.

[141] BOBRAKOV 91 searched for anomalous magnetic interactions between polarized electrons expected from the exchange of a massless pseudoscalar boson (arion). A limit $x_e^2 < 2\times10^{-4}$ (95%CL) is found for the effective anomalous magneton parametrized as $x_e(G_F/8\pi\sqrt{2})^{1/2}$.

[142] ALBRECHT 90E limits are for B($\tau \to \ell X^0$)/B($\tau \to \ell\nu\nu$). Valid for m_{X^0} < 100 MeV. The limits rise to 7.1% (for μ), 5.0% (for e) for m_{X^0} = 500 MeV.

[143] ATIYA 90 limit is for $m_{X^0} = 0$. The limit B $< 1\times10^{-8}$ holds for m_{X^0} < 95 MeV. For the reduction of the limit due to finite lifetime of X^0, see their Fig. 3.

[144] BOLTON 88 limit corresponds to $F > 3.1\times10^9$ GeV, which does not depend on the chirality property of the coupling.

[145] CHANDA 88 find v_T < 10 MeV for the weak-triplet Higgs vacuum expectation value in Gelmini-Roncadelli model, and $v_S > 5.8\times10^6$ GeV in the singlet Majoron model.

[146] CHOI 88 used the observed neutrino flux from the supernova SN 1987A to exclude the neutrino Majoron Yukawa coupling h in the range $2\times10^{-5} < h < 3\times10^{-4}$ for the interaction $L_{\rm int} = \frac{1}{2}ih\overline{\psi}^c_\nu\gamma_5\psi_\nu\phi_X$. For several families of neutrinos, the limit applies for $(\Sigma h_i^4)^{1/4}$.

[147] PICCIOTTO 88 limit applies when m_{X^0} < 55 MeV and τ_{X^0} > 2ns, and it decreases to 4×10^{-7} at m_{X^0} = 125 MeV, beyond which no limit is obtained.

[148] GOLDMAN 87 limit corresponds to $F > 2.9\times10^9$ GeV for the family symmetry breaking scale from the Lagrangian $L_{\rm int} = (1/F)\psi_\mu\gamma^\mu(a+b\gamma_5)\psi_e\partial_\mu\phi_{X^0}$ with $a^2+b^2 = 1$. This is not as sensitive as the limit $F > 9.9\times10^9$ GeV derived from the search for $\mu^+ \to e^+X^0$ by JODIDIO 86, but does not depend on the chirality property of the coupling.

[149] Limits are for $\Gamma(\mu \to eX^0)/\Gamma(\mu \to e\nu\nu)$. Valid when m_{X^0} = 0–93.4, 98.1–103.5 MeV.

[150] EICHLER 86 looked for $\mu^+ \to e^+X^0$ followed by $X^0 \to e^+e^-$. Limits on the branching fraction depend on the mass and and lifetime of X^0. The quoted limits are valid when $\tau_{X^0} \lesssim 3.\times10^{-10}$ s if the decays are kinematically allowed.

[151] JODIDIO 86 corresponds to $F > 9.9\times10^9$ GeV for the family symmetry breaking scale with the parity-conserving effective Lagrangian $L_{\rm int} = (1/F)\,\overline{\psi}_\mu\gamma^\mu\psi_e\partial^\mu\phi_{X^0}$.

[152] BALTRUSAITIS 85 search for light Goldstone boson(X^0) of broken U(1). CL = 95% limits are B($\tau \to \mu^+X^0$)/B($\tau \to \mu^+\nu\nu$) <0.125 and B($\tau \to e^+X^0$)/B($\tau \to e^+\nu\nu$) <0.04. Inferred limit for the symmetry breaking scale is m >3000 TeV.

[153] The primordial heavy neutrino must decay into ν and familon, f_A, early so that the red-shifted decay products are below critical density, see their table. In addition, $K \to \pi f_A$ and $\mu \to e f_A$ are unseen. Combining these excludes $m_{\text{heavy}\nu}$ between 5×10^{-5} and 5×10^{-4} MeV (μ decay) and $m_{\text{heavy}\nu}$ between 5×10^{-5} and 0.1 MeV (K-decay).

Majoron Searches in Neutrinoless Double β Decay

Limits are for the half-life of neutrinoless $\beta\beta$ decay with a Majoron emission.

No experiment currently claims any such evidence. Only the best or comparable limits for each isotope are reported. Also see the reviews ZUBER 98 and FAESSLER 98B.

$t_{1/2}$(10^{21} yr)	CL%	ISOTOPE	TRANSITION	METHOD	DOCUMENT ID	
>7200	**90**	**^{128}Te**		**CNTR**	[154] BERNATOW...	92
• • • We do not use the following data for averages, fits, limits, etc. • • •						
> 27	90	^{100}Mo	$0\nu1\chi$	NEMO-3	[155] ARNOLD	06
> 15	90	^{82}Se	$0\nu1\chi$	NEMO-3	[156] ARNOLD	06
> 14	90	^{100}Mo	$0\nu1\chi$	NEMO-3	[157] ARNOLD	04
> 12	90	^{82}Se	$0\nu1\chi$	NEMO-3	[158] ARNOLD	04
> 2.2	90	^{130}Te	$0\nu1\chi$	Cryog. det.	[159] ARNABOLDI	03
> 0.9	90	^{130}Te	$0\nu2\chi$	Cryog. det.	[160] ARNABOLDI	03
> 8	90	^{116}Cd	$0\nu1\chi$	$CdWO_4$ scint.	[161] DANEVICH	03
> 0.8	90	^{116}Cd	$0\nu2\chi$	$CdWO_4$ scint.	[162] DANEVICH	03
> 500	90	^{136}Xe	$0\nu\chi$	Liquid Xe Scint.	[163] BERNABEI	02D
> 5.8	90	^{100}Mo	$0\nu\chi$	ELEGANT V	[164] FUSHIMI	02
> 0.32	90	^{100}Mo	$0\nu\chi$	Liq. Ar ioniz.	[165] ASHITKOV	01
> 0.0035	90	^{160}Gd	$0\nu\chi$	$^{160}Gd_2SiO_5$:Ce	[166] DANEVICH	01
> 0.013	90	^{160}Gd	$0\nu2\chi$	$^{160}Gd_2SiO_5$:Ce	[167] DANEVICH	01
> 2.3	90	^{82}Se	$0\nu\chi$	NEMO 2	[168] ARNOLD	00
> 0.31	90	^{96}Zr	$0\nu\chi$	NEMO 2	[169] ARNOLD	00
> 0.63	90	^{82}Se	$0\nu2\chi$	NEMO 2	[170] ARNOLD	00
> 0.063	90	^{96}Zr	$0\nu2\chi$	NEMO 2	[170] ARNOLD	00
> 0.16	90	^{100}Mo	$0\nu2\chi$	NEMO 2	[170] ARNOLD	00
> 2.4	90	^{82}Se	$0\nu\chi$	NEMO 2	[171] ARNOLD	98
> 7.2	90	^{136}Xe	$0\nu2\chi$	TPC	[172] LUESCHER	98
> 7.91	90	^{76}Ge		SPEC	[173] GUENTHER	96
> 17	90	^{76}Ge		CNTR	BECK	93

[154] BERNATOWICZ 92 studied double-β decays of ^{128}Te and ^{130}Te, and found the ratio $\tau(^{130}\text{Te})/\tau(^{128}\text{Te}) = (3.52 \pm 0.11)\times10^{-4}$ in agreement with relatively stable theoretical predictions. The bound is based on the requirement that Majoron-emitting decay cannot be larger than the observed double-beta rate of ^{128}Te of $(7.7\pm0.4)\times10^{24}$ year. We calculated 90% CL limit as $(7.7{-}1.28\times0.4{=}7.2)\times10^{24}$.

[155] ARNOLD 06 use ^{100}Mo data taken with the NEMO-3 tracking detector. The reported limit corresponds to $\langle g_{\nu\chi}\rangle < (0.4\text{–}1.8)\times10^{-4}$ using a range of matrix element calculations. Supersedes ARNOLD 04.

[156] NEMO-3 tracking calorimeter is used in ARNOLD 06 . Reported half-life limit for ^{82}Se corresponds to $\langle g_{\nu\chi}\rangle < (0.66\text{–}1.9)\times10^{-4}$ using a range of matrix element calculations. Supersedes ARNOLD 04.

[157] ARNOLD 04 use the NEMO-3 tracking detector. The limit corresponds to $\langle g_{\nu\chi}\rangle <$ (0.5–0.9)10^{-4} using the matrix elements of SIMKOVIC 99, STOICA 01 and CIVITARESE 03.

[158] ARNOLD 04 use the NEMO-3 tracking detector. The limit corresponds to $\langle g_{\nu\chi}\rangle <$ (0.7–1.6)10^{-4} using the matrix elements of SIMKOVIC 99, STOICA 01 and CIVITARESE 03.

[159] Supersedes ALESSANDRELLO 00. Array of TeO_2 crystals in high resolution cryogenic calorimeter. Some enriched in ^{130}Te. Derive $\langle g_{\nu\chi}\rangle <$ 17–33 $\times10^{-5}$ depending on matrix element.

[160] Supersedes ALESSANDRELLO 00. Cryogenic calorimeter search.

[161] Limit for the $0\nu\chi$ decay with Majoron emission of ^{116}Cd using enriched $CdWO_4$ scintillators. $\langle g_{\nu\chi}\rangle <$ 4.6–8.1 $\times10^{-5}$ depending on the matrix element. Supersedes DANEVICH 00.

[162] Limit for the $0\nu2\chi$ decay of ^{116}Cd. Supersedes DANEVICH 00.

[163] BERNABEI 02D obtain limit for $0\nu\chi$ decay with Majoron emission of ^{136}Xe using liquid Xe scintillation detector. They derive $\langle g_{\nu\chi}\rangle <$ 2.0–3.0 $\times10^{-5}$ with several nuclear matrix elements.

[164] Replaces TANAKA 93. FUSHIMI 02 derive half-life limit for the $0\nu\chi$ decay by means of tracking calorimeter ELEGANT V. Considering various matrix element calculations, a range of limits for the Majoron-neutrino coupling is given: $\langle g_{\nu\chi}\rangle$ <(6.3–360) $\times10^{-5}$.

[165] ASHITKOV 01 result for $0\nu\chi$ of ^{100}Mo is less stringent than ARNOLD 00.

[166] DANEVICH 01 obtain limit for the $0\nu\chi$ decay with Majoron emission of ^{160}Gd using Gd_2SiO_5:Ce crystal scintillators.

[167] DANEVICH 01 obtain limit for the $0\nu2\chi$ decay with 2 Majoron emission of ^{160}Gd.

[168] ARNOLD 00 reports limit for the $0\nu\chi$ decay with Majoron emission derived from tracking calorimeter NEMO 2. Using ^{82}Se source: $\langle g_{\nu\chi}\rangle < 1.6\times10^{-4}$. Matrix element from GUENTHER 96.

[169] Using ^{96}Zr source: $\langle g_{\nu\chi}\rangle < 2.6\times10^{-4}$. Matrix element from ARNOLD 99.

[170] ARNOLD 00 reports limit for the $0\nu2\chi$ decay with two Majoron emission derived from tracking calorimeter NEMO 2.

[171] ARNOLD 98 determine the limit for $0\nu_\chi$ decay with Majoron emission of ^{82}Se using the NEMO-2 tracking detector. They derive $\langle g_{\nu_\chi}\rangle < 2.3\text{–}4.3\times10^{-4}$ with several nuclear matrix elements.

[172] LUESCHER 98 report a limit for the 0ν decay with Majoron emission of ^{136}Xe using Xe TPC. This result is more stringent than BARABASH 89. Using the matrix elements of ENGEL 88, they obtain a limit on $\langle g_{\nu\chi} \rangle$ of 2.0×10^{-4}.

[173] See Table 1 in GUENTHER 96 for limits on the Majoron coupling in different models.

Invisible A^0 (Axion) MASS LIMITS from Astrophysics and Cosmology

$v_1 = v_2$ is usually assumed (v_i = vacuum expectation values). For a review of these limits, see RAFFELT 91 and TURNER 90. In the comment lines below, D and K refer to DFSZ and KSVZ axion types, discussed in the above minireview.

VALUE (eV)	*CL%*	*DOCUMENT ID*	*TECN*	*COMMENT*
• • • We do not use the following data for averages, fits, limits, etc. • • •				
< 1.02	95	[174] HANNESTAD 08	COSM	K, hot dark matter
< 1.2	95	[175] HANNESTAD 07	COSM	K, hot dark matter
< 0.42	95	[176] MELCHIORRI 07A	COSM	K, hot dark matter
< 1.05	95	[177] HANNESTAD 05A	COSM	K, hot dark matter
3 to 20		[178] MOROI 98	COSM	K, hot dark matter
< 0.007		[179] BORISOV 97	ASTR	D, neutron star
< 4		[180] KACHELRIESS 97	ASTR	D, neutron star cooling
$<(0.5–6) \times 10^{-3}$		[181] KEIL 97	ASTR	SN 1987A
< 0.018		[182] RAFFELT 95	ASTR	D, red giant
< 0.010		[183] ALTHERR 94	ASTR	D, red giants, white dwarfs
		[184] CHANG 93	ASTR	K, SN 1987A
< 0.01		WANG 92	ASTR	D, white dwarf
< 0.03		WANG 92C	ASTR	D, C-O burning
none 3–8		[185] BERSHADY 91	ASTR	D, K, intergalactic light
<10		[186] KIM 91C	COSM	D, K, mass density of the universe, supersymmetry
		[187] RAFFELT 91B	ASTR	D,K, SN 1987A
$< 1 \times 10^{-3}$		[188] RESSELL 91	ASTR	K, intergalactic light
none 10^{-3}–3		BURROWS 90	ASTR	D,K, SN 1987A
		[189] ENGEL 90	ASTR	D,K, SN 1987A
< 0.02		[190] RAFFELT 90D	ASTR	D, red giant
$< 1 \times 10^{-3}$		[191] BURROWS 89	ASTR	D,K, SN 1987A
$<(1.4–10) \times 10^{-3}$		[192] ERICSON 89	ASTR	D,K, SN 1987A
$< 3.6 \times 10^{-4}$		[193] MAYLE 89	ASTR	D,K, SN 1987A
<12		CHANDA 88	ASTR	D, Sun
$< 1 \times 10^{-3}$		RAFFELT 88	ASTR	D,K, SN 1987A
		[194] RAFFELT 88B	ASTR	red giant
< 0.07		FRIEMAN 87	ASTR	D, red giant
< 0.7		[195] RAFFELT 87	ASTR	K, red giant
$< 2–5$		TURNER 87	COSM	K, thermal production
< 0.01		[196] DEARBORN 86	ASTR	D, red giant
< 0.06		RAFFELT 86	ASTR	D, red giant
< 0.7		[197] RAFFELT 86	ASTR	K, red giant
< 0.03		RAFFELT 86B	ASTR	D, white dwarf
< 1		[198] KAPLAN 85	ASTR	K, red giant
$< 0.003–0.02$		IWAMOTO 84	ASTR	D, K, neutron star
$> 1 \times 10^{-5}$		ABBOTT 83	COSM	D,K, mass density of the universe
$> 1 \times 10^{-5}$		DINE 83	COSM	D,K, mass density of the universe
< 0.04		ELLIS 83B	ASTR	D, red giant
$> 1 \times 10^{-5}$		PRESKILL 83	COSM	D,K, mass density of the universe
< 0.1		BARROSO 82	ASTR	D, red giant
< 1		[199] FUKUGITA 82	ASTR	D, stellar cooling
< 0.07		FUKUGITA 82B	ASTR	D, red giant

[174] This is an update of HANNESTAD 07 including 5 years of WMAP data.

[175] This is an update of HANNESTAD 05A with new cosmological data, notably WMAP (3 years) and baryon acoustic oscillations (BAO). Lyman-α data are left out, in contrast to HANNESTAD 05A and MELCHIORRI 07A, because it is argued that systematic errors are large. It uses Bayesian statistics and marginalizes over a possible neutrino hot dark matter component.

[176] MELCHIORRI 07A is analogous to HANNESTAD 05A, with updated cosmological data, notably WMAP (3 years). Uses Bayesian statistics and marginalizes over a possible neutrino hot dark matter component. Leaving out Lyman-α data, a conservative limit is 1.4 eV.

[177] HANNESTAD 05A puts an upper limit on the mass of hadronic axion because in this mass range it would have been thermalized and contribute to the hot dark matter component of the universe. The limit is based on the CMB anisotropy from WMAP, SDSS large scale structure, Lyman α, and the prior Hubble parameter from HST Key Project. A χ^2 statistic is used. Neutrinos are assumed not to contribute to hot dark matter.

[178] MOROI 98 points out that a KSVZ axion of this mass range (see CHANG 93) can be a viable hot dark matter of Universe, as long as the model-dependent $g_{A\gamma}$ is accidentally small enough as originally emphasized by KAPLAN 85; see Fig. 1.

[179] BORISOV 97 bound is on the axion-electron coupling $g_{ae} < 1 \times 10^{-13}$ from the photo-production of axions off of magnetic fields in the outer layers of neutron stars.

[180] KACHELRIESS 97 bound is on the axion-electron coupling $g_{ae} < 1 \times 10^{-10}$ from the production of axions in strongly magnetized neutron stars. The authors also quote a stronger limit, $g_{ae} < 9 \times 10^{-13}$ which is strongly dependent on the strength of the magnetic field in white dwarfs.

[181] KEIL 97 uses new measurements of the axial-vector coupling strength of nucleons, as well as a reanalysis of many-body effects and pion-emission processes in the core of the neutron star, to update limits on the invisible-axion mass.

[182] RAFFELT 95 reexamined the constraints on axion emission from red giants due to the axion-electron coupling. They improve on DEARBORN 86 by taking into proper account degeneracy effects in the bremsstrahlung rate. The limit comes from requiring the red giant core mass at helium ignition not to exceed its standard value by more than 5% (0.025 solar masses).

[183] ALTHERR 94 bound is on the axion-electron coupling $g_{ae} < 1.5 \times 10^{-13}$, from energy loss via axion emission.

[184] CHANG 93 updates ENGEL 90 bound with the Kaplan-Manohar ambiguity in $z = m_u/m_d$ (see the Note on the Quark Masses in the Quark Particle Listings). It leaves the window $f_A = 3 \times 10^5$–3×10^6 GeV open. The constraint from Big-Bang Nucleosynthesis is satisfied in this window as well.

[185] BERSHADY 91 searched for a line at wave length from 3100–8300 Å expected from 2γ decays of relic thermal axions in intergalactic light of three rich clusters of galaxies.

[186] KIM 91C argues that the bound from the mass density of the universe will change drastically for the supersymmetric models due to the entropy production of saxion (scalar component in the axionic chiral multiplet) decay. Note that it is an *upperbound* rather than a lowerbound.

[187] RAFFELT 91B argue that previous SN 1987A bounds must be relaxed due to corrections to nucleon bremsstrahlung processes.

[188] RESSELL 91 uses absence of any intracluster line emission to set limit.

[189] ENGEL 90 rule out $10^{-10} \lesssim g_{AN} \lesssim 10^{-3}$, which for a hadronic axion with EMC motivated axion-nucleon couplings corresponds to 2.5×10^{-3} eV $\lesssim m_{A^0} \lesssim 2.5 \times 10^4$ eV. The constraint is loose in the middle of the range, i.e. for $g_{AN} \sim 10^{-6}$.

[190] RAFFELT 90D is a re-analysis of DEARBORN 86.

[191] The region $m_{A^0} \gtrsim 2$ eV is also allowed.

[192] ERICSON 89 considered various nuclear corrections to axion emission in a supernova core, and found a reduction of the previous limit (MAYLE 88) by a large factor.

[193] MAYLE 89 limit based on naive quark model couplings of axion to nucleons. Limit based on couplings motivated by EMC measurements is 2–4 times weaker. The limit from axion-electron coupling is weak: see HATSUDA 88B.

[194] RAFFELT 88B derives a limit for the energy generation rate by exotic processes in helium-burning stars $\epsilon < 100$ erg g^{-1} s^{-1}, which gives a firmer basis for the axion limits based on red giant cooling.

[195] RAFFELT 87 also gives a limit $g_{A\gamma} < 1 \times 10^{-10}$ GeV^{-1}.

[196] DEARBORN 86 also gives a limit $g_{A\gamma} < 1.4 \times 10^{-11}$ GeV^{-1}.

[197] RAFFELT 86 gives a limit $g_{A\gamma} < 1.1 \times 10^{-10}$ GeV^{-1} from red giants and $< 2.4 \times 10^{-9}$ GeV^{-1} from the sun.

[198] KAPLAN 85 says $m_{A^0} < 23$ eV is allowed for a special choice of model parameters.

[199] FUKUGITA 82 gives a limit $g_{A\gamma} < 2.3 \times 10^{-10}$ GeV^{-1}.

Search for Relic Invisible Axions

Limits are for $[G_{A\gamma\gamma}/m_{A^0}]^2 \rho_A$ where $G_{A\gamma\gamma}$ denotes the axion two-photon coupling, $L_{\rm int} = \frac{G_{A\gamma\gamma}}{4} \phi_A F_{\mu\nu} \widetilde{F}^{\mu\nu} = G_{A\gamma\gamma} \phi_A \mathbf{E}\cdot\mathbf{B}$, and ρ_A is the axion energy density near the earth.

VALUE	*CL%*	*DOCUMENT ID*	*TECN*	*COMMENT*
• • • We do not use the following data for averages, fits, limits, etc. • • •				
$<1.9 \times 10^{-43}$	97.7	[200] DUFFY 06	CNTR	$m_{A^0} = 1.98–2.17 \times 10^{-6}$ eV
$<5.5 \times 10^{-43}$	90	[201] ASZTALOS 04	CNTR	$m_{A^0} = 1.9–3.3 \times 10^{-6}$ eV
		[202] KIM 98	THEO	
$<2 \times 10^{-41}$		[203] HAGMANN 90	CNTR	$m_{A^0} = (5.4–5.9)10^{-6}$ eV
$<1.3 \times 10^{-42}$	95	[204] WUENSCH 89	CNTR	$m_{A^0} = (4.5–10.2)10^{-6}$ eV
$<2 \times 10^{-41}$	95	[204] WUENSCH 89	CNTR	$m_{A^0} = (11.3–16.3)10^{-6}$ eV

[200] DUFFY 06 used the upgraded detector of ASZTALOS 04, while assuming a smaller velocity dispersion than the isothermal model as in Eq. (8) of their paper. See Fig. 10 of their paper on the axion mass dependence of the limit.

[201] ASZTALOS 04 looked for a conversion of halo axions to microwave photons in magnetic field. At 90% CL, the KSVZ axion cannot have a local halo density more than 0.45 GeV/cm^3 in the quoted mass range. See Fig. 7 of their paper on the axion mass dependence of the limit.

[202] KIM 98 calculated the axion-to-photon couplings for various axion models and compared them to the HAGMANN 90 bounds. This analysis demonstrates a strong model dependence of $G_{A\gamma\gamma}$ and hence the bound from relic axion search.

[203] HAGMANN 90 experiment is based on the proposal of SIKIVIE 83.

[204] WUENSCH 89 looks for condensed axions near the earth that could be converted to photons in the presence of an intense electromagnetic field via the Primakoff effect, following the proposal of SIKIVIE 83. The theoretical prediction with $[G_{A\gamma\gamma}/m_{A^0}]^2 = 2 \times 10^{-14}$ MeV^{-4} (the three generation DFSZ model) and $\rho_A = 300$ MeV/cm^3 that makes up galactic halos gives $(G_{A\gamma\gamma}/m_{A^0})^2\ \rho_A = 4 \times 10^{-44}$. Note that our definition of $G_{A\gamma\gamma}$ is $(1/4\pi)$ smaller than that of WUENSCH 89.

Invisible A^0 (Axion) Limits from Photon Coupling

Limits are for the axion-two-photon coupling $G_{A\gamma\gamma}$ defined by $L = G_{A\gamma\gamma} \phi_A \mathbf{E}\cdot\mathbf{B}$. Related limits from astrophysics can be found in the "Invisible A^0 (Axion) Mass Limits from Astrophysics and Cosmology" section.

VALUE (GeV^{-1})	*CL%*	*DOCUMENT ID*	*TECN*	*COMMENT*
• • • We do not use the following data for averages, fits, limits, etc. • • •				
$<3.5 \times 10^{-7}$	99.7	[205] CHOU 08		$m_{A^0} < 0.5$ meV
$<5 \times 10^{-7}$		[206] ZAVATTINI 08		$m_{A^0} < 1$ meV
$<8.8 \times 10^{-11}$	95	[207] ANDRIAMON... 07	CAST	$m_{A^0} < 0.02$ eV
$<1.25 \times 10^{-6}$	95	[208] ROBILLIARD 07		$m_{A^0} < 1$ meV

$2–5 \times 10^{-6}$		[209] ZAVATTINI	06		$m_{A^0} = 1–1.5$ meV
$<1.1 \times 10^{-9}$	95	[210] INOUE	02		$m_{A^0} = 0.05–0.27$ eV
$<2.78 \times 10^{-9}$	95	[211] MORALES	02B		$m_{A^0} <1$ keV
$<1.7 \times 10^{-9}$	90	[212] BERNABEI	01B		$m_{A^0} <100$ eV
$<1.5 \times 10^{-4}$	90	[213] ASTIER	00B	NOMD	$m_{A^0} <40$ eV
		[214] MASSO	00	THEO	induced γ coupling
$<2.7 \times 10^{-9}$	95	[215] AVIGNONE	98	SLAX	$m_{A^0} < 1$ keV
$<6.0 \times 10^{-10}$	95	[216] MORIYAMA	98		$m_{A^0} < 0.03$ eV
$<3.6 \times 10^{-7}$	95	[217] CAMERON	93		$m_{A^0} < 10^{-3}$ eV, optical rotation
$<6.7 \times 10^{-7}$	95	[218] CAMERON	93		$m_{A^0} < 10^{-3}$ eV, photon regeneration
$<3.6 \times 10^{-9}$	99.7	[219] LAZARUS	92		$m_{A^0} < 0.03$ eV
$<7.7 \times 10^{-9}$	99.7	[219] LAZARUS	92		$m_{A^0} = 0.03–0.11$ eV
$<7.7 \times 10^{-7}$	99	[220] RUOSO	92		$m_{A^0} < 10^{-3}$ eV
$<2.5 \times 10^{-6}$		[221] SEMERTZIDIS	90		$m_{A^0} < 7 \times 10^{-4}$ eV

[205] CHOU 08 perform a variable-baseline photon regeneration experiment. See their Fig. 3 for mass-dependent limits. Excludes the PVLAS result of ZAVATTINI 06.

[206] ZAVATTINI 08 is an upgrade of ZAVATTINI 06, see their Fig. 8 for mass-dependent limits. They now exclude the parameter range where ZAVATTINI 06 had seen a positive signature.

[207] ANDRIAMONJE 07 looked for Primakoff conversion of solar axions in 9T superconducting magnet into X-rays. Supersedes ZIOUTAS 05.

[208] ROBILLIARD 07 perform a photon regeneration experiment with a pulsed laser and pulsed magnetic field. See their Fig. 4 for mass-dependent limits. Excludes the PVLAS result of ZAVATTINI 06 with a CL exceeding 99.9%.

[209] ZAVATTINI 06 propagate a laser beam in a magnetic field and observe dichroism and birefringence effects that could be attributed to an axion-like particle. This result is now excluded by ROBILLIARD 07, ZAVATTINI 08, and CHOU 08.

[210] INOUE 02 looked for Primakoff conversion of solar axions in 4T superconducting magnet into X ray.

[211] MORALES 02B looked for the coherent conversion of solar axions to photons via the Primakoff effect in Germanium detector.

[212] BERNABEI 01B looked for Primakoff coherent conversion of solar axions into photons via Bragg scattering in NaI crystal in DAMA dark matter detector.

[213] ASTIER 00B looked for production of axions from the interaction of high-energy photons with the horn magnetic field and their subsequent re-conversion to photons via the interaction with the NOMAD dipole magnetic field.

[214] MASSO 00 studied limits on axion-proton coupling using the induced axion-photon coupling through the proton loop and CAMERON 93 bound on the axion-photon coupling using optical rotation. They obtained the bound $g_p^2/4\pi < 1.7 \times 10^{-9}$ for the coupling $g_p \overline{p} \gamma_5 p \phi_A$.

[215] AVIGNONE 98 result is based on the coherent conversion of solar axions to photons via the Primakoff effect in a single crystal germanium detector.

[216] Based on the conversion of solar axions to X-rays in a strong laboratory magnetic field.

[217] Experiment based on proposal by MAIANI 86.

[218] Experiment based on proposal by VANBIBBER 87.

[219] LAZARUS 92 experiment is based on proposal found in VANBIBBER 89.

[220] RUOSO 92 experiment is based on the proposal by VANBIBBER 87.

[221] SEMERTZIDIS 90 experiment is based on the proposal of MAIANI 86. The limit is obtained by taking the noise amplitude as the upper limit. Limits extend to $m_{A^0} = 4 \times 10^{-3}$ where $G_{A\gamma\gamma} < 1 \times 10^{-4}$ GeV^{-1}.

Limit on Invisible A^0 (Axion) Electron Coupling

The limit is for $G_{Aee} \partial_\mu \phi_A e \gamma^\mu \gamma_5 e$ in GeV^{-1}, or equivalently, the dipole-dipole potential $\frac{G_{Aee}^2}{4\pi} \left((\boldsymbol{\sigma}_1 \cdot \boldsymbol{\sigma}_2) - 3(\boldsymbol{\sigma}_1 \cdot \boldsymbol{n}) (\boldsymbol{\sigma}_2 \cdot \boldsymbol{n}) \right)/r^3$ where $\boldsymbol{n}=\boldsymbol{r}/r$.

The limits below apply to invisible axion of $m_A \leq 10^{-6}$ eV.

VALUE (GeV^{-1})	*CL%*	*DOCUMENT ID*		*TECN*	*COMMENT*
• • • We do not use the following data for averages, fits, limits, etc. • • •					
$<5.3 \times 10^{-5}$	66	[222] NI	94		Induced magnetism
$<6.7 \times 10^{-5}$	66	[222] CHUI	93		Induced magnetism
$<3.6 \times 10^{-4}$	66	[223] PAN	92		Torsion pendulum
$<2.7 \times 10^{-5}$	95	[222] BOBRAKOV	91		Induced magnetism
$<1.9 \times 10^{-3}$	66	[224] WINELAND	91	NMR	
$<8.9 \times 10^{-4}$	66	[223] RITTER	90		Torsion pendulum
$<6.6 \times 10^{-5}$	95	[222] VOROBYOV	88		Induced magnetism

[222] These experiments measured induced magnetization of a bulk material by the spin-dependent potential generated from other bulk material with aligned electron spins, where the magnetic field is shielded with superconductor.

[223] These experiments used a torsion pendulum to measure the potential between two bulk matter objects where the spins are polarized but without a net magnetic field in either of them.

[224] WINELAND 91 looked for an effect of bulk matter with aligned electron spins on atomic hyperfine splitting using nuclear magnetic resonance.

Invisible A^0 (Axion) Limits from Nucleon Coupling

Limits are for the axion mass in eV.

VALUE (eV)	*CL%*	*DOCUMENT ID*		*TECN*	*COMMENT*
• • • We do not use the following data for averages, fits, limits, etc. • • •					
		[225] BELLINI	08	CNTR	Solar axion
		[226] ADELBERGER	07		Test of Newton's law
<360	90	[227] DERBIN	07	CNTR	Solar axion
<216	95	[228] NAMBA	07	CNTR	Solar axion
$< 1.6 \times 10^4$	90	[229] DERBIN	05	CNTR	Solar axion
<400	95	[230] LJUBICIC	04	CNTR	Solar axion
$< 3.2 \times 10^4$	95	[231] KRCMAR	01	CNTR	Solar axion
<745	95	[232] KRCMAR	98	CNTR	Solar axion

[225] BELLINI 08 consider solar axions emitted in the M1 transition of ^{7}Li* (478 keV) and look for a peak at 478 keV in the energy spectra of the Counting Test Facility (CTF), a Borexino prototype. For $m_{A^0} < 450$ keV they find mass-dependent limits on products of axion couplings to photons, electrons, and nucleons.

[226] ADELBERGER 07 use precision tests of Newton's law to constrain a force contribution from the exchange of two pseudoscalars. See their Fig. 5 for limits on the pseudoscalar coupling to nucleons, relevant for m_{A^0} below about 1 meV.

[227] DERBIN 07 is analogous to KRCMAR 98.

[228] NAMBA 07 is analogous to KRCMAR 98.

[229] DERBIN 05 bound is based on the same principle as KRCMAR 01.

[230] LJUBICIC 04 looked for ejection of K-shell electrons by the axioelectric effect of 14.4 keV solar axions in a Germanium detector. The limit assumes the hadronic axion model and the same solar axion flux as in KRCMAR 98 and KRCMAR 01.

[231] KRCMAR 01 looked for solar axions emitted by the M1 transition of ^{7}Li after the electron capture by ^{7}Be and the emission of 384 keV line neutrino, using their resonant capture on ^{7}Li in the laboratory. The mass bound assumes $m_u/m_d = 0.56$ and the flavor-singlet axial-vector matrix element S=0.4.

[232] KRCMAR 98 looked for solar axions emitted by the M1 transition of thermally excited ^{57}Fe nuclei in the Sun, using their possible resonant capture on ^{57}Fe in the laboratory, following MORIYAMA 95B. The mass bound assumes m_u/m_d=0.56 and the flavor-singlet axial-vector matrix element $S=3F-D \simeq 0.5$.

Axion Limits from T-violating Medium-Range Forces

The limit is for the coupling g in a T-violating potential between nucleons or nucleon and electron of the form $V = \frac{g \hbar^2}{8\pi m_p} (\boldsymbol{\sigma} \cdot \hat{\boldsymbol{r}}) \left(\frac{1}{r^2} + \frac{m_A c}{\hbar r} \right) e^{-m_A c r/\hbar}$

VALUE	*DOCUMENT ID*		*TECN*	*COMMENT*
• • • We do not use the following data for averages, fits, limits, etc. • • •				
	[233] BAESSLER	07		ultracold neutrons
	[234] HECKEL	06		torsion pendulum
	[235] NI	99		paramagnetic Tb F_3
	[236] POSPELOV	98	THEO	neutron EDM
	[237] YOUDIN	96		
	[238] RITTER	93		torsion pendulum
	[239] VENEMA	92		nuclear spin-precession frequencies
	[240] WINELAND	91	NMR	

[233] BAESSLER 07 use the observation of quantum states of ultracold neutrons in the Earth's gravitational field to constrain g for an interaction range 1 μm–a few mm. See their Fig. 3 for results.

[234] HECKEL 06 studied the influence of unpolarized bulk matter, including the laboratory's surroundings or the Sun, on a torsion pendulum containing about 9×10^{22} polarized electrons. See their Fig. 4 for limits on g as a function of interaction range.

[235] NI 99 searched for a T-violating medium-range force acting on paramagnetic Tb F_3 salt. See their Fig. 1 for the result.

[236] POSPELOV 98 studied the possible contribution of T-violating Medium-Range Force to the neutron electric dipole moment, which is possible when axion interactions violate CP. The size of the force among nucleons must be smaller than gravity by a factor of 2×10^{-10} (1 cm/λ_A), where $\lambda_A = \hbar/m_A c$.

[237] YOUDIN 96 compared the precession frequencies of atomic ^{199}Hg and Cs when a large mass is positioned near the cells, relative to an applied magnetic field. See Fig. 3 for their limits.

[238] RITTER 93 studied the influence of bulk mass with polarized electons on an unpolarized torsion pendulum, providing limits in the interaction range from 1 to 100 cm.

[239] VENEMA 92 looked for an effect of Earth's gravity on nuclear spin-precession frequencies of ^{199}Hg and ^{201}Hg atoms.

[240] WINELAND 91 looked for an effect of bulk matter with aligned electron spins on atomic hyperfine resonances in stored ^{9}Be$^+$ ions using nuclear magnetic resonance.

REFERENCES FOR Searches for Axions (A^0) and Other Very Light Bosons

BELLINI	08	EPJ C54 61	G. Bellini *et al.*	(Borexino Collab.)
CHOU	08	PRL 100 080402	A.S. Chou *et al.*	(GammeV Collab.)
HANNESTAD	08	JCAP 0804 019	S. Hannestad *et al.*	
ZAVATTINI	08	PR D77 032006	E. Zavattini *et al.*	(PVLAS Collab.)
ADELBERGER	07	PRL 98 131104	E.G. Adelberger *et al.*	
ANDRIAMON...	07	JCAP 0704 010	S. Andriamonje *et al.*	(CAST Collab.)
BAESSLER	07	PR D75 075006	S. Baessler *et al.*	
CHANG	07	PR D75 052004	H.M. Chang *et al.*	(TEXONO Collab.)
DERBIN	07	JETPL 85 12	A.V. Derbin *et al.*	
HANNESTAD	07	JCAP 0708 015	S. Hannestad *et al.*	
JAIN	07	JPG 34 129	P.L. Jain, G. Singh	
LESSA	07	PR D75 094001	A.P. Lessa, O.L.G. Peres	
MELCHIORRI	07A	PR D76 041303R	A. Melchiorri, O. Mena, A. Slosar	
NAMBA	07	PL B645 398	T. Namba	
ROBILLIARD	07	PRL 99 190403	C. Robilliard *et al.*	
ARNOLD	06	NP A765 483	R. Arnold *et al.*	(NEMO-3 Collab.)
DUFFY	06	PR D74 012006	L.D. Duffy *et al.*	
HECKEL	06	PRL 97 021603	B.R. Heckel *et al.*	
ZAVATTINI	06	PRL 96 110406	E. Zavattini *et al.*	(PVLAS Collab.)
DERBIN	05	JETPL 81 365	A.V. Derbin *et al.*	
		Translated from ZETFP 81 453.		
HANNESTAD	05A	JCAP 0507 002	S. Hannestad, A. Mirizzi, G. Raffelt	
PARK	05	PRL 94 021801	H.K. Park *et al.*	(FNAL HyperCP Collab.)
ZIOUTAS	05	PRL 94 121301	K. Zioutas *et al.*	(CAST Collab.)
ADLER	04	PR D70 037102	S. Adler *et al.*	(BNL E787 Collab.)
ANISIMOVSK...	04	PRL 93 031801	V.V. Anisimovsky *et al.*	(BNL E949 Collab.)
ARNOLD	04	JETPL 80 377	R. Arnold *et al.*	(NEMO3 Detector Collab.)
		Translated from ZETFP 80 429.		

ASZTALOS	04	PR D69 011101R	S.J. Asztalos *et al.*
LJUBICIC	04	PL B599 143	A. Ljubicic *et al.*
ARNABOLDI	03	PL B557 167	C. Arnaboldi *et al.*
CIVITARESE	03	NP A729 867	O. Civitarese, J. Suhonen
DANEVICH	03	PR C68 035501	F.A. Danevich *et al.*
ADLER	02C	PL B537 211	S. Adler *et al.* (BNL E787 Collab.)
BADERT...	02	PL B542 29	A. Badertscher *et al.*
BERNABEI	02D	PL B546 23	R. Bernabei *et al.* (DAMA Collab.)
DERBIN	02	PAN 65 1302	A.V. Derbin *et al.*
		Translated from YAF 65 1335.	
FUSHIMI	02	PL B531 190	K. Fushimi *et al.* (ELEGANT V Collab.)
INOUE	02	PL B536 18	Y. Inoue *et al.*
MORALES	02B	ASP 16 325	A. Morales *et al.* (COSME Collab.)
ADLER	01	PR D63 032004	S. Adler *et al.* (BNL E787 Collab.)
AMMAR	01B	PRL 87 271801	R. Ammar *et al.* (CLEO Collab.)
ASHITKOV	01	JETPL 74 529	V.D. Ashitkov *et al.*
		Translated from ZETFP 74 601.	
BERNABEI	01B	PL B515 6	R. Bernabei *et al.* (DAMA Collab.)
DANEVICH	01	NP A694 375	F.A. Danevich *et al.*
DEBOER	01	JPG 27 L29	F.W.N. de Boer *et al.*
KRCMAR	01	PR D64 115016	M. Krcmar *et al.*
STOICA	01	NP A694 269	S. Stoica, H.V. Klapdor-Kleingrothous
ALESSAND...	00	PL B486 13	A. Alessandrello *et al.*
ARNOLD	00	NP A678 341	R. Arnold *et al.*
ASTIER	00B	PL B479 371	P. Astier *et al.* (NOMAD Collab.)
DANEVICH	00	PR C62 045501	F.A. Danevich *et al.*
MASSO	00	PR D61 011701R	E. Masso
ARNOLD	99	NP A658 299	R. Arnold *et al.* (NEMO Collab.)
NI	99	PRL 82 2439	W.-T. Ni *et al.*
SIMKOVIC	99	PR C60 055502	F. Simkovic *et al.*
ALTEGOER	98	PL B428 197	J. Altegoer *et al.*
ARNOLD	98	NP A636 209	R. Arnold *et al.* (NEMO-2 Collab.)
AVIGNONE	98	PRL 81 5068	F.T. Avignone *et al.* (Solar Axion Experiment)
DIAZ	98	NP B527 44	M.A. Diaz *et al.*
FAESSLER	98B	JPG 24 2139	A. Faessler, F. Simkovic
KIM	98	PR D58 055006	J.E. Kim
KRCMAR	98	PL B442 38	M. Krcmar *et al.*
LUESCHER	98	PL B434 407	R. Luescher *et al.*
MORIYAMA	98	PL B434 147	S. Moriyama *et al.*
MOROI	98	PL B440 69	T. Moroi, H. Murayama
POSPELOV	98	PR D58 097703	M. Pospelov
ZUBER	98	PRPL 305 295	K. Zuber
AHMAD	97	PRL 78 618	I. Ahmad *et al.* (APEX Collab.)
BORISOV	97	JETP 83 868	A.V. Borisov, V.Y. Grishinia (MOSU)
DEBOER	97C	JPG 23 L85	F.W.N. de Boer *et al.*
KACHELRIESS	97	PR D56 1313	M. Kachelriess, C. Wilke, G. Wunner (BOCH)
KEIL	97	PR D56 2419	W. Keil *et al.*
KITCHING	97	PRL 79 4079	P. Kitching *et al.* (BNL E787 Collab.)
LEINBERGER	97	PL B394 16	U. Leinberger *et al.* (ORANGE Collab.)
ADLER	96	PRL 76 1421	S. Adler *et al.* (BNL E787 Collab.)
AMSLER	96B	ZPHY C70 219	C. Amsler *et al.* (Crystal Barrel Collab.)
GANZ	96	PL B389 4	R. Ganz *et al.* (GSI, HEID, FRAN, JAGL+)
GUENTHER	96	PR D54 3641	M. Gunther *et al.* (MPIH, SASSO)
KAMEL	96	PL B368 291	S. Kamel (SHAMS)
MITSUI	96	EPL 33 111	T. Mitsui *et al.* (TOKY)
YOUDIN	96	PRL 77 2170	A.N. Youdin *et al.* (AMHT, WASH)
ALTMANN	95	ZPHY C68 221	M. Altmann *et al.* (MUNT, LAPP, CPPM)
BALEST	95	PR D51 2053	R. Balest *et al.* (CLEO Collab.)
BASSOMPIE...	95	PL B355 584	G. Bassompierre *et al.* (LAPP, LCGT, LYON)
MAENO	95	PL B351 574	T. Maeno *et al.* (TOKY)
MORIYAMA	95B	PRL 75 3222	S. Moriyama
RAFFELT	95	PR D51 1495	G. Raffelt, A. Weiss (MPIM, MPIA)
SKALSEY	95	PR D51 6292	M. Skalsey, R.S. Conti (MICH)
TSUNODA	95	EPL 30 273	T. Tsunoda *et al.* (TOKY)
ADACHI	94	PR A49 3201	S. Adachi *et al.* (TMU)
ALTHERR	94	ASP 2 175	T. Altherr, E. Petitgirard, T. del Rio Gaztelurrutia
AMSLER	94B	PL B333 271	C. Amsler *et al.* (Crystal Barrel Collab.)
ASAI	94	PL B323 90	S. Asai *et al.* (TOKY)
MEIJERDREES	94	PR D49 4937	M.R. Drees *et al.* (BRCO, OREG, TRIU)
NI	94	Physica B194 153	W.T. Ni *et al.* (NTHU)
VO	94	PR C49 1551	D.T. Vo *et al.* (ISU, LBL, LLNL, UCD)
ATIYA	93	PRL 70 2521	M.S. Atiya *et al.* (BNL E787 Collab.)
Also		PRL 71 305 (erratum)	M.S. Atiya *et al.* (BNL E787 Collab.)
ATIYA	93B	PR D48 R1	M.S. Atiya *et al.* (BNL E787 Collab.)
BASSOMPIE...	93	EPL 22 239	G. Bassompierre *et al.* (LAPP, TORI, LYON)
BECK	93	PRL 70 2853	M. Beck *et al.* (MPIH, KIAE, SASSO)
CAMERON	93	PR D47 3707	R.E. Cameron *et al.* (ROCH, BNL, FNAL+)
CHANG	93	PL B316 51	S. Chang, K. Choi
CHUI	93	PRL 71 3247	T.C.P. Chui, W.T. Ni (NTHU)
MINOWA	93	PRL 71 4120	M. Minowa *et al.* (TOKY)
NG	93	PR D48 2941	K.W. Ng (AST)
RITTER	93	PRL 70 701	R.C. Ritter *et al.*
TANAKA	93	PR D48 5412	J. Tanaka, H. Ejiri (OSAK)
ALLIEGRO	92	PRL 68 278	C. Alliegro *et al.* (BNL, FNAL, PSI+)
ATIYA	92	PRL 69 733	M.S. Atiya *et al.* (BNL, LANL, PRIN+)
BERNATOW...	92	PRL 69 2341	T. Bernatowicz *et al.* (WUSL, TATA)
BLUEMLEIN	92	IJMP A7 3835	J. Blumlein *et al.* (BERL, BUDA, JINR+)
HALLIN	92	PR D45 3955	A.L. Hallin *et al.* (PRIN)
HENDERSON	92C	PRL 69 1733	S.D. Henderson *et al.* (YALE, BNL)
HICKS	92	PL B276 423	K.H. Hicks, D.E. Alburger (OHIO, BNL)
LAZARUS	92	PRL 69 2333	D.M. Lazarus *et al.* (BNL, ROCH, FNAL)
MEIJERDREES	92	PRL 68 3845	R. Meijer Drees *et al.* (SINDRUM I Collab.)
PAN	92	MPL A7 1287	S.S. Pan, W.T. Ni, S.C. Chen (NTHU)
RUOSO	92	ZPHY C56 505	G. Ruoso *et al.* (ROCH, BNL, FNAL, TRST)
SKALSEY	92	PRL 68 456	M. Skalsey, J.J. Kolata (MICH, NDAM)
VENEMA	92	PRL 68 135	B.J. Venema *et al.*
WANG	92	MPL A7 1497	J. Wang (ILL)
WANG	92C	PL B291 97	J. Wang (ILL)
WU	92	PRL 69 1729	X.Y. Wu *et al.* (BNL, YALE, CUNY)
AKOPYAN	91	PL B272 443	M.V. Akopyan *et al.* (INRM)
ASAI	91	PRL 66 2440	S. Asai *et al.* (ICEPP)
BERSHADY	91	PRL 66 1398	M.A. Bershady, M.T. Ressell, M.S. Turner (CHIC+)
BLUEMLEIN	91	ZPHY C51 341	J. Blumlein *et al.* (BERL, BUDA, JINR+)
BOBRAKOV	91	JETPL 53 294	V.F. Bobrakov *et al.* (PNPI)
		Translated from ZETFP 53 283.	
BROSS	91	PRL 67 2942	A.D. Bross *et al.* (FNAL, ILL)
KIM	91C	PRL 67 3465	J.E. Kim (SEOUL)
RAFFELT	91	PRPL 198 1	G.G. Raffelt (MPIM)
RAFFELT	91B	PRL 67 2605	G. Raffelt, D. Seckel (MPIM, BART)
RESSELL	91	PR D44 3001	M.T. Ressell (CHIC, FNAL)
TRZASKA	91	PL B269 54	W.H. Trzaska *et al.* (TAMU)
TSERTOS	91	PL B266 259	H. Tsertos *et al.* (ILLG, GSI)
WALKER	91	APJ 376 51	T.P. Walker *et al.* (HSCA, OSU, CHIC+)
WIDMANN	91	ZPHY A340 209	E. Widmann *et al.* (STUT, GSI, STUTM)
WINELAND	91	PRL 67 1735	D.J. Wineland *et al.* (NBSB)
ALBRECHT	90E	PL B246 278	H. Albrecht *et al.* (ARGUS Collab.)
ANTREASYAN	90C	PL B251 204	D. Antreasyan *et al.* (Crystal Ball Collab.)
ASANUMA	90	PL B237 588	T. Asanuma *et al.* (TOKY)
ATIYA	90	PRL 64 21	M.S. Atiya *et al.* (BNL E787 Collab.)
ATIYA	90B	PRL 65 1188	M.S. Atiya *et al.* (BNL E787 Collab.)
BAUER	90	NIM B50 300	W. Bauer *et al.* (STUT, VILL, GSI)
BURROWS	90	PR D42 3297	A. Burrows, M.T. Ressell, M.S. Turner (ARIZ+)
DEBOER	90	JPG 16 L1	F.W.N. de Boer, J. Lehmann, J. Steyaert (LOUV)
ENGEL	90	PRL 65 960	J. Engel, D. Seckel, A.C. Hayes (BART, LANL)
GNINENKO	90	PL B237 287	S.N. Gninenko *et al.* (INRM)
GUO	90	PR D41 2924	R. Guo *et al.* (NIU, LANL, FNAL, CASE+)
HAGMANN	90	PR D42 1297	C. Hagmann *et al.* (FLOR)
JUDGE	90	PRL 65 972	S.M. Judge *et al.* (ILLG, GSI)
RAFFELT	90D	PR D41 1324	G.G. Raffelt (MPIM)
RITTER	90	PR D42 977	R.C. Ritter *et al.* (VIRG)
SEMERTZIDIS	90	PRL 64 2988	Y.K. Semertzidis *et al.* (ROCH, BNL, FNAL+)
TSUCHIAKI	90	PL B236 81	M. Tsuchiaki *et al.* (ICEPP)
TURNER	90	PRPL 197 67	M.S. Turner (FNAL)
BARABASH	89	PL B223 273	A.S. Barabash *et al.* (ITEP, INRM)
BINI	89	PL B221 99	M. Bini *et al.* (FIRZ, CERN, AARH)
BURROWS	89	PR D39 1020	A. Burrows, M.S. Turner, R.P. Brinkmann (ARIZ+)
Also		PRL 60 1797	M.S. Turner (FNAL, EFI)
DEBOER	89B	PRL 62 2639	F.W.N. de Boer, R. van Dantzig (ANIK)
ERICSON	89	PL B219 507	T.E.O. Ericson, J.F. Mathiot (CERN, IPN)
FAISSNER	89	ZPHY C44 557	H. Faissner *et al.* (AACH3, BERL, PSI)
FOX	89	PR C39 288	J.D. Fox *et al.* (FSU)
MAYLE	89	PL B219 515	R. Mayle *et al.* (LLL, CERN, MINN, FNAL+)
Also		PL B203 188	R. Mayle *et al.* (LLL, CERN, MINN, FNAL+)
MINOWA	89	PRL 62 1091	H. Minowa *et al.* (ICEPP)
ORITO	89	PRL 63 597	S. Orito *et al.* (ICEPP)
PERKINS	89	PRL 62 2638	D.H. Perkins (OXF)
TSERTOS	89	PR D40 1397	H. Tsertos *et al.* (GSI, ILLG)
VANBIBBER	89	PR D39 2089	K. van Bibber *et al.* (LLL, TAMU, LBL)
WUENSCH	89	PR D40 3153	W.U. Wuensch *et al.* (ROCH, BNL, FNAL)
Also		PRL 59 839	S. de Panfilis *et al.* (ROCH, BNL, FNAL)
AVIGNONE	88	PR D37 618	F.T. Avignone *et al.* (PRIN, SCUC, ORNL+)
BJORKEN	88	PR D38 3375	J.D. Bjorken *et al.* (FNAL, SLAC, VPI)
BLINOV	88	SJNP 47 563	A.E. Blinov *et al.* (NOVO)
		Translated from YAF 47 889.	
BOLTON	88	PR D38 2077	R.D. Bolton *et al.* (LANL, STAN, CHIC+)
Also		PRL 56 2461	R.D. Bolton *et al.* (LANL, STAN, CHIC+)
Also		PRL 57 3241	D. Grosnick *et al.* (CHIC, LANL, STAN+)
CHANDA	88	PR D37 2714	R. Chanda, J.F. Nieves, P.B. Pal (UMD, UPR+)
CHOI	88	PR D37 3225	K. Choi *et al.* (JHU)
CONNELL	88	PRL 60 2242	S.H. Connell *et al.* (WITW)
DATAR	88	PR C37 250	V.M. Datar *et al.* (IPN)
DEBOER	88	PRL 61 1274	F.W.N. de Boer, R. van Dantzig (ANIK)
Also		PRL 62 2644 (erratum)	F.W.N. de Boer, R. van Dantzig (ANIK)
Also		PRL 62 2638	D.H. Perkins (OXF)
Also		PRL 62 2639	F.W.N. de Boer, R. van Dantzig (ANIK)
DEBOER	88C	JPG 14 L131	F.W.N. de Boer *et al.* (LOUV)
DOEHNER	88	PR D38 2722	J. Dohner *et al.* (HEIDP, ANL, ILLG)
EL-NADI	88	PRL 61 1271	M. el Nadi, O.E. Badawy (CAIR)
ENGEL	88	PR C37 731	J. Engel, P. Vogel, M.R. Zirnbauer
FAISSNER	88	ZPHY C37 231	H. Faissner *et al.* (AACH3, BERL, SIN)
HATSUDA	88B	PL B203 469	T. Hatsuda, M. Yoshimura (KEK)
LORENZ	88	PL B214 10	E. Lorenz *et al.* (MPIM, PSI)
MAYLE	88	PL B203 188	R. Mayle *et al.* (LLL, CERN, MINN, FNAL+)
PICCIOTTO	88	PR D37 1131	C.E. Picciotto *et al.* (TRIU, CNRC)
RAFFELT	88	PRL 60 1793	G. Raffelt, D. Seckel (UCB, LLL, UCSC)
RAFFELT	88B	PR D37 549	G.G. Raffelt, D.S.P. Dearborn (UCB, LLL)
SAVAGE	88	PR D37 1134	M.J. Savage, B.W. Filippone, L.W. Mitchell (CIT)
TSERTOS	88	PL B207 273	A. Tsertos *et al.* (GSI, ILLG)
TSERTOS	88B	ZPHY A331 103	A. Tsertos *et al.* (GSI, ILLG)
VANKLINKEN	88	PL B205 223	J. van Klinken *et al.* (GRON, GSI)
VANKLINKEN	88B	PRL 60 2442	J. van Klinken (GRON)
VONWIMMER...	88	PRL 60 2443	U. von Wimmersperg (BNL)
VOROBYOV	88	PL B208 146	P.V. Vorobiev, Y.I. Gitarts (NOVO)
DRUZHININ	87	ZPHY C37 1	V.P. Druzhinin *et al.* (NOVO)
FRIEMAN	87	PR D36 2201	J.A. Frieman, S. Dimopoulos, M.S. Turner (SLAC+)
GOLDMAN	87	PR D36 1543	T. Goldman *et al.* (LANL, CHIC, STAN+)
KORENCHE...	87	SJNP 46 192	S.M. Korenchenko *et al.* (JINR)
		Translated from YAF 46 313.	
MAIER	87	ZPHY A326 527	K. Maier *et al.* (STUT, GSI)
MILLS	87	PR D36 707	A.P. Mills, J. Levy (BELL)
RAFFELT	87	PR D36 2211	G.G. Raffelt, D.S.P. Dearborn (LLL, UCB)
RIORDAN	87	PRL 59 755	E.M. Riordan *et al.* (ROCH, CIT+)
TURNER	87	PRL 59 2489	M.S. Turner (FNAL, EFI)
VANBIBBER	87	PRL 59 759	K. van Bibber *et al.* (LLL, CIT, MIT+)
VONWIMMER...	87	PRL 59 266	U. von Wimmersperg *et al.* (WITW)
ALBRECHT	86D	PL B179 403	H. Albrecht *et al.* (ARGUS Collab.)
BADIER	86	ZPHY C31 21	J. Badier *et al.* (NA3 Collab.)
BOWCOCK	86	PRL 56 2676	T.J.V. Bowcock *et al.* (CLEO Collab.)
BROWN	86	PRL 57 2101	C.N. Brown *et al.* (FNAL, WASH, KYOT+)
BRYMAN	86B	PRL 57 2787	D.A. Bryman, E.T.H. Clifford (TRIU)
DAVIER	86	PL B180 295	M. Davier, J. Jeanjean, H. Nguyen Ngoc (LALO)
DEARBORN	86	PRL 56 26	D.S.P. Dearborn, D.N. Schramm, G. Steigman (LLL+)
EICHLER	86	PL B175 101	R.A. Eichler *et al.* (SINDRUM Collab.)
HALLIN	86	PRL 57 2105	A.L. Hallin *et al.* (PRIN)
JODIDIO	86	PR D34 1967	A. Jodidio *et al.* (LBL, NWES, TRIU)
Also		PR D37 237 (erratum)	A. Jodidio *et al.* (LBL, NWES, TRIU)
KETOV	86	JETPL 44 146	S.N. Ketov *et al.* (KIAE)
		Translated from ZETFP 44 114.	
KOCH	86	NC 96A 182	H.R. Koch, O.W.B. Schult (JULI)
KONAKA	86	PRL 57 659	A. Konaka *et al.* (KYOT, KEK)
MAGERAS	86	PRL 56 2672	G. Mageras *et al.* (MPIM, COLU, STON)
MAIANI	86	PL B175 359	L. Maiani, R. Petronzio, E. Zavattini (CERN)
PECCEI	86	PL B172 435	R.D. Peccei, T.T. Wu, T. Yanagida (DESY)
RAFFELT	86	PR D33 897	G.G. Raffelt (MPIM)
RAFFELT	86B	PL 166B 402	G.G. Raffelt (MPIM)
SAVAGE	86B	PRL 57 178	M.J. Savage *et al.* (CIT)
AMALDI	85	PL 153B 444	U. Amaldi *et al.* (CERN)
ANANEV	85	SJNP 41 585	V.D. Ananev *et al.* (JINR)
		Translated from YAF 41 912.	
BALTRUSAIT...	85	PRL 55 1842	R.M. Baltrusaitis *et al.* (Mark III Collab.)
BERGSMA	85	PL 157B 458	F. Bergsma *et al.* (CHARM Collab.)
KAPLAN	85	NP B260 215	D.B. Kaplan (HARV)
IWAMOTO	84	PRL 53 1198	N. Iwamoto (UCSB, WUSL)
YAMAZAKI	84	PRL 52 1089	T. Yamazaki *et al.* (INUS, KEK)
ABBOTT	83	PL 120B 133	L.F. Abbott, P. Sikivie (BRAN, FLOR)
ALAM	83	PR D27 1665	M.S. Alam *et al.* (VAND, CORN, ITHA, HARV+)
CARBONI	83	PL 123B 349	G. Carboni, W. Dahme (CERN, MUNI)
CAVAIGNAC	83	PL 121B 193	J.F. Cavaignac *et al.* (ISNG, LAPP)
DICUS	83	PR D28 1778	D.A. Dicus, V.L. Teplitz (TEXA, UMD)
DINE	83	PL 120B 137	M. Dine, W. Fischler (IAS, PENN)
ELLIS	83B	NP B223 252	J. Ellis, K.A. Olive (CERN)
FAISSNER	83	PR D28 1198	H. Faissner *et al.* (AACH)
FAISSNER	83B	PR D28 1787	H. Faissner *et al.* (AACH3)
FRANK	83B	PR D28 1790	J.S. Frank *et al.* (LANL, YALE, LBL+)
HOFFMAN	83	PR D28 660	C.M. Hoffman *et al.* (LANL, ARZS)
NICZYPORUK	83	ZPHY C17 197	B. Niczyporuk *et al.* (LENA Collab.)
PRESKILL	83	PL 120B 127	J. Preskill, M.B. Wise, F. Wilczek (HARV, UCSBT)
SIKIVIE	83	PRL 51 1415	P. Sikivie (FLOR)
Also		PRL 52 695 (erratum)	P. Sikivie (FLOR)
ALEKSEEV	82	JETP 55 591	E.A. Alekseeva *et al.* (KIAE)
		Translated from ZETF 82 1007.	
ALEKSEEV	82B	JETPL 36 116	G.D. Alekseev *et al.* (MOSU, JINR)
		Translated from ZETFP 36 94.	

ASANO 82 PL 113B 195 Y. Asano *et al.* (KEK, TOKY, INUS, OSAK)
BARROSO 82 PL 116B 247 A. Barroso, G.C. Branco (LISB)
DATAR 82 PL 114B 63 V.M. Datar *et al.* (BHAB)
EDWARDS 82 PRL 48 903 C. Edwards *et al.* (Crystal Ball Collab.)
FETSCHER 82 JPG 8 L147 W. Fetscher (ETH)
FUKUGITA 82 PRL 48 1522 M. Fukugita, S. Watamura, M. Yoshimura (KEK)
FUKUGITA 82B PR D26 1840 M. Fukugita, S. Watamura, M. Yoshimura (KEK)
LEHMANN 82 PL 115B 270 P. Lehmann *et al.* (SACL)
RAFFELT 82 PL 119B 323 G. Raffelt, L. Stodolsky (MPIM)
SIVERTZ 82 PR D26 717 J.M. Sivertz *et al.* (CUSB Collab.)
ZEHNDER 82 PL 110B 419 A. Zehnder, K. Gabathuler, J.L. Vuilleumier (ETH+)
ASANO 81B PL 107B 159 Y. Asano *et al.* (KEK, TOKY, INUS, OSAK)
BARROSO 81 PL 106B 91 A. Barroso, N.C. Mukhopadhyay (SIN)
FAISSNER 81 ZPHY C10 95 H. Faissner *et al.* (AACH3)
FAISSNER 81B PL 103B 234 H. Faissner *et al.* (AACH3)
KIM 81 PL 105B 55 B.R. Kim, C. Stamm (AACH3)
VUILLEUMIER 81 PL 101B 341 J.L. Vuilleumier *et al.* (CIT, MUNI)
ZEHNDER 81 PL 104B 494 A. Zehnder (ETH)
FAISSNER 80 PL 96B 201 H. Faissner *et al.* (AACH3)
JACQUES 80 PR D21 1206 P.F. Jacques *et al.* (RUTG, STEV, COLU)
SOUKAS 80 PRL 44 564 A. Soukas *et al.* (BNL, HARV, ORNL, PENN)
BECHIS 79 PRL 42 1511 D.J. Bechis *et al.* (UMD, COLU, AFRR)
CALAPRICE 79 PR D20 2708 F.P. Calaprice *et al.* (PRIN)
COTEUS 79 PRL 42 1438 P. Coteus *et al.* (COLU, ILL, BNL)
DISHAW 79 PL 85B 142 J.P. Dishaw *et al.* (SLAC, CIT)
ZHITNITSKII 79 SJNP 29 517 A.R. Zhitnitsky, Y.I. Skovpen (NOVO)
Translated from YAF 29 1001.
ALIBRAN 78 PL 74B 134 P. Alibran *et al.* (Gargamelle Collab.)
ASRATYAN 78B PL 79B 497 A.E. Asratyan *et al.* (ITEP, SERP)
BELLOTTI 78 PL 76B 223 E. Bellotti, E. Fiorini, L. Zanotti (MILA)
BOSETTI 78B PL 74B 143 P.C. Bosetti *et al.* (BEBC Collab.)
DICUS 78C PR D18 1829 D.A. Dicus *et al.* (TEXA, VPI, STAN)
DONNELLY 78 PR D18 1607 T.W. Donnelly *et al.* (STAN)
Also PRL 37 315 F. Reines, H.S. Gurr, H.W. Sobel (UCI)
Also PRL 33 179 H.S. Gurr, F. Reines, H.W. Sobel (UCI)
HANSL 78D PL 74B 139 T. Hansl *et al.* (CDHS Collab.)
MICELMAC... 78 LNC 21 441 G.V. Mitselmakher, B. Pontecorvo (JINR)
MIKAELIAN 78 PR D18 3605 K.O. Mikaelian (FNAL, NWES)
SATO 78 PTP 60 1942 K. Sato (KYOT)
VYSOTSKII 78 JETPL 27 502 M.I. Vysotsky *et al.* (ASCI)
Translated from ZETFP 27 533.
YANG 78 PRL 41 523 T.C. Yang (MASA)
PECCEI 77 PR D16 1791 R.D. Peccei, H.R. Quinn (STAN, SLAC)
Also PRL 38 1440 R.D. Peccei, H.R. Quinn (STAN, SLAC)
REINES 76 PRL 37 315 F. Reines, H.S. Gurr, H.W. Sobel (UCI)
GURR 74 PRL 33 179 H.S. Gurr, F. Reines, H.W. Sobel (UCI)
ANAND 53 PRSL A22 183 B.M. Anand

OTHER RELATED PAPERS

SREDNICKI 85 NP B260 689 M. Srednicki (UCSB)
BARDEEN 78 PL 74B 229 W.A. Bardeen, S.-H.H. Tye (FNAL)